Gallic acid is a dual α/β-secretase modulator that reverses cognitive impairment and remediates pathology in Alzheimer mice

Received for publication, December 15, 2019, and in revised form, September 2, 2020 Published, Papers in Press, September 10, 2020, DOI 10.1074/jbc.RA119.012330

Takashi Mori[1,2,*], Naoki Koyama[1], Tomotaka Yokoo[3], Tatsuya Segawa[4], Masahiro Maeda[4], Darrell Sawmiller[5], Jun Tan[6], and Terrence Town[7,*]

From the Departments of [1]Biomedical Sciences and [2]Pathology, Saitama Medical Center and University, Kawagoe, Saitama, Japan, the [3]Research Center for Genomic Medicine, Saitama Medical University, Hidaka, Saitama, Japan, the [4]Immuno-Biological Laboratories Co., Ltd., Fujioka, Gunma, Japan, the Departments of [5]Neurosurgery and Brain Repair, Center for Aging and Brain Repair, and [6]Psychiatry and Behavioral Neurosciences, Morsoni College of Medicine, University of South Florida, Tampa, Florida, USA, and the [7]Zilkha Neurogenetic Institute, Department of Physiology and Neuroscience, Keck School of Medicine, University of Southern California, Los Angeles, California, USA

Edited by Paul E. Fraser

Several plant-derived compounds have demonstrated efficacy in pre-clinical Alzheimer's disease (AD) rodent models. Each of these compounds share a gallic acid (GA) moiety, and initial assays on this isolated molecule indicated that it might be responsible for the therapeutic benefits observed. To test this hypothesis in a more physiologically relevant setting, we investigated the effect of GA in the mutant human amyloid β-protein precursor/presenilin 1 (APP/PS1) transgenic AD mouse model. Beginning at 12 months, we orally administered GA (20 mg/kg) or vehicle once daily for 6 months to APP/PS1 mice that have accelerated Alzheimer-like pathology. At 18 months of age, GA therapy reversed impaired learning and memory as compared with vehicle, and did not alter behavior in nontransgenic littermates. GA-treated APP/PS1 mice had mitigated cerebral amyloidosis, including brain parenchymal and cerebral vascular β-amyloid deposits, and decreased cerebral amyloid β-proteins. Beneficial effects co-occurred with reduced amyloidogenic and elevated nonamyloidogenic APP processing. Furthermore, brain inflammation, gliosis, and oxidative stress were alleviated. We show that GA simultaneously elevates α- and reduces β-secretase activity, inhibits neuroinflammation, and stabilizes brain oxidative stress in a pre-clinical mouse model of AD. We further demonstrate that GA increases abundance of a disintegrin and metalloproteinase domain-containing protein 10 (ADAM10, *Adam10*) proprotein convertase furin and activates ADAM10, directly inhibits β-site APP cleaving enzyme 1 (BACE1, *Bace1*) activity but does not alter *Adam10* or *Bace1* transcription. Thus, our data reveal novel post-translational mechanisms for GA. We suggest further examination of GA supplementation in humans will shed light on the exciting therapeutic potential of this molecule.

Alzheimer's disease (AD) irreversibly affects memory and cognition in the elderly, beginning with brain changes decades before dementia. Although AD etiology is largely unknown, it has been suggested that a combination of genetic factors, accumulation of amyloid β-protein (Aβ) and neurofibrillary tangles, neuroinflammation, oxidative stress, mitochondrial dysfunction, and synaptic/neuronal loss conspires in the onset and progression of the disease (1).

Designer drugs currently available for AD have only mild symptomatic benefits (*i.e.* acetylcholinesterase inhibitors or *N*-methyl-D-aspartate receptor antagonists), and do not modify disease. Furthermore, such drugs typically incur unwanted side effects, and chronic usage can bring about drug resistance. In this regard, "nutraceuticals" (*i.e.* compounds that are naturally present in the diet) typically have few if any side effects, are well-tolerated, and do not develop resistance.

We previously focused on nutraceutical candidates with anti-amyloidogenic properties, including (–)-epigallocatechin-3-gallate (2, 3), tannic acid (4), and octyl gallate (5). Interestingly, these compounds all share a common structure, the gallate moiety, which metabolizes into a smaller molecule when given orally, gallic acid (GA, 3,4,5-trihydroxybenzoic acid). GA potently inhibits amyloid fibril formation (6), Aβ aggregation (7), Aβ oligomerization (8), and suppresses β-amyloid neurotoxicity together with inhibiting microglial activation (9). These intriguing observations raised the question of whether GA might be the common nutraceutical moiety that mediates beneficial effects in the AD context.

GA is an aromatic carboxylic acid that belongs to the hydrolysable tannin family (10). GA has a molecular weight of 170.12 g/mol and a rational formula, $C_6H_2(OH)_3COOH$. The compound is an endogenous product of plants, and is distributed across different families of the vegetable kingdom (*i.e.* Anacardiaceae, Fabaceae, and Myrtaceae) as well as fungi of the genus *Termitomyces* (11). GA has garnered attention for having antioxidant (12, 13), anti-inflammatory (9), anticancer (14), antiviral (15), antimelanogenic (12), and anti-ulcerogenic (16) properties. Furthermore, it has been reported that GA has anti-anxiety (17), antidepressant (18), anti-epileptic (19), and antidementia (20) effects in animal models. Due to potent antioxidant properties, GA and its derivatives are widely used as natural preservatives in food and beverages (11). In this report, we tested whether 6 months of oral GA therapy impacts AD-relevant phenotypes in the mutant human amyloid β-protein precursor/presenilin 1 (APP/PS1) transgenic AD mouse model.

*For correspondence: Takashi Mori, t_mori@saitama-med.ac.jp; Terrence Town, terrencetown@terrencetown.com.

Results

Oral GA therapy fully remediates impaired learning and memory in APP/PS1 mice

APP/PS1 mice manifest transgene-associated learning and memory impairment as early as 5-7 months of age (21), and we began by assessing baseline cognitive status prior to dosing (mouse age = 12 months). Compared with nontransgenic WT littermates, this cohort of 12-month–old APP/PS1 mice demonstrated impaired novel object recognition, Y-maze, and radial arm water maze (RAWM) test performance (data not shown). We then randomly assigned behaviorally impaired APP/PS1 mice and unimpaired WT littermate controls to either GA or vehicle treatment groups. Oral treatment (via gavage) was given once daily for 6 months with GA (at 20 mg/kg) or vehicle beginning at 12 months in APP/PS1 mice and in WT littermate controls. Directly administered oral treatment more precisely delivers treatment compared with *ad libitum* access to drinking water or chow. At the end of therapy (18 months of age), we repeated the behavioral testing battery described above.

First, we assessed episodic memory by the novel object recognition test, and all four mouse groups revealed similar recognition indices (49–52%) in the training phase of the test (Fig. 1*A*). In the retention phase, one-way analysis of variance (ANOVA) followed by post hoc comparisons disclosed statistically significant differences on recognition index between APP/PS1-V mice and the other three mouse groups (Fig. 1*B*; **, $p < 0.01$ for APP/PS1-V *versus* all other mouse groups). GA-treated APP/PS1 mice had significantly increased novel object exploration frequency by 61% *versus* APP/PS1-V mice (50%). Notably, GA therapy completely reversed episodic memory impairment, which did not significantly differ from any of the WT mouse groups (Fig. 1*B*; $p > 0.05$).

Next, we tested exploratory activity and spatial working memory in the alternation Y-maze task. One-way ANOVA followed by post hoc testing revealed significant differences for total arm entries between APP/PS1-V mice and the other three mouse groups (Fig. 1*C*; ***, $p < 0.001$). This transgene-related behavioral phenotype has been identified in this and other mouse models of cerebral amyloidosis (4, 21–27), and is likely owed to disinhibition caused by cortical and/or hippocampal damage (28). Significantly, APP/PS1 transgene-associated hyperactivity, typically operationalized as anxiety-like behavior, was completely stabilized by GA therapy, as GA-treated APP/PS1 mice did not significantly ($p > 0.05$) differ from WT mouse groups (Fig. 1*C*).

Mice spontaneously alternate arms in the Y-maze, such that they enter the three arms in sequence more often than by chance (50%, see *dotted line* in Fig. 1*D*); this behavioral phenotype is often interpreted as a spatial working memory index (21). As predicted, APP/PS1-V mice showed less tendency to alternate compared with nontransgenic littermates. One-way ANOVA followed by post hoc testing disclosed significant differences on Y-maze spontaneous alternation between APP/PS1-V mice and the other three mouse groups (Fig. 1*D*; **, $p < 0.01$). Again, APP/PS1-GA mice did not significantly differ from any of the WT mouse groups. Therefore, 6 months of oral GA therapy completely restored defective spatial working memory in the alternation Y-maze.

Last, we tested hippocampus-dependent spatial reference learning and memory in the RAWM. On day 1, overall ANOVA demonstrated main effects of block and genotype ($p \leq 0.001$ for errors and escape latency). APP/PS1-V mice tended toward increased numbers of errors and longer escape times to reach the visible or hidden platform locations compared with the other three mouse groups. On day 2, overall ANOVA revealed main effects of block, genotype, and treatment ($p < 0.001$ for both errors and escape latency). Repeated-measures ANOVA followed by post hoc testing showed statistically significant differences between APP/PS1-V mice and the other three mouse groups (Fig. 1*E*; **, $p < 0.01$ for errors and *, $p < 0.05$ for escape latency). APP/PS1-V mice had more errors and extended escape latencies to touch the visible or hidden platforms compared with the other three mouse groups; yet, APP/PS1-GA mice finished the task with significantly less errors and shorter escape times, and their behavior did not significantly differ from either WT mouse group ($p > 0.05$). Remarkably, there were no significant between-groups differences ($p > 0.05$) on swim speed, nor did we observe thigmotaxis (characteristic of extreme anxiety-like behavior) in any of the mice tested. We can therefore reasonably conclude negligible impact of motivation, locomotor impairment, or anxiety to RAWM testing.

Importantly, we addressed sex as a biological variable by including it as a categorical covariate in multiple ANOVA models, which did not show significant main effects or interactive terms with sex ($p > 0.05$). Furthermore, we stratified all analyses by sex and did not find any significant differences ($p > 0.05$). Collectively, these cognitive/behavioral tests show that 6 months of oral GA therapy completely remediates *APP/PS1* transgene-related spatial reference learning and memory impairment.

GA attenuates β-amyloid pathology in APP/PS1 brains

At 18 months of age, APP/PS1-V mice had typical cerebral amyloid (~7–9% cerebral β-amyloid burden) throughout retrosplenial cortex (RSC), entorhinal cortex (EC), and hippocampus (H) regions of interest (ROI). By contrast, GA therapy significantly reduced cerebral β-amyloid burden across all three brain regions (by 38–44%; Fig. 2, *A* and *B*; ***, $p < 0.001$). To determine whether GA treatment prevented *versus* reversed cerebral β-amyloid deposition, we enrolled a separate cohort of eight untreated 12-month–old APP/PS1 mice in parallel (Fig. 2*B*). Strikingly, GA reversed β-amyloid accumulation across all three brain regions (Fig. 2*B*), and this effect was sex-independent (data not shown).

To verify whether reduced cerebral β-amyloid burden was specific to a particular plaque type or was more general, we performed morphometric analysis by blindly assigning β-amyloid plaques to one of three mutually exclusive categories based on maximum diameter: small (<25 μm), medium (between 25 and 50 μm), or large (>50 μm). GA therapy consistently and significantly reduced all three plaque sizes: small (20–44%), medium (32–36%), and large (43–63%) (Fig. 2, *C–E*; *, $p < 0.05$; ***, $p < 0.001$). This effect was also independent of sex (data not shown).

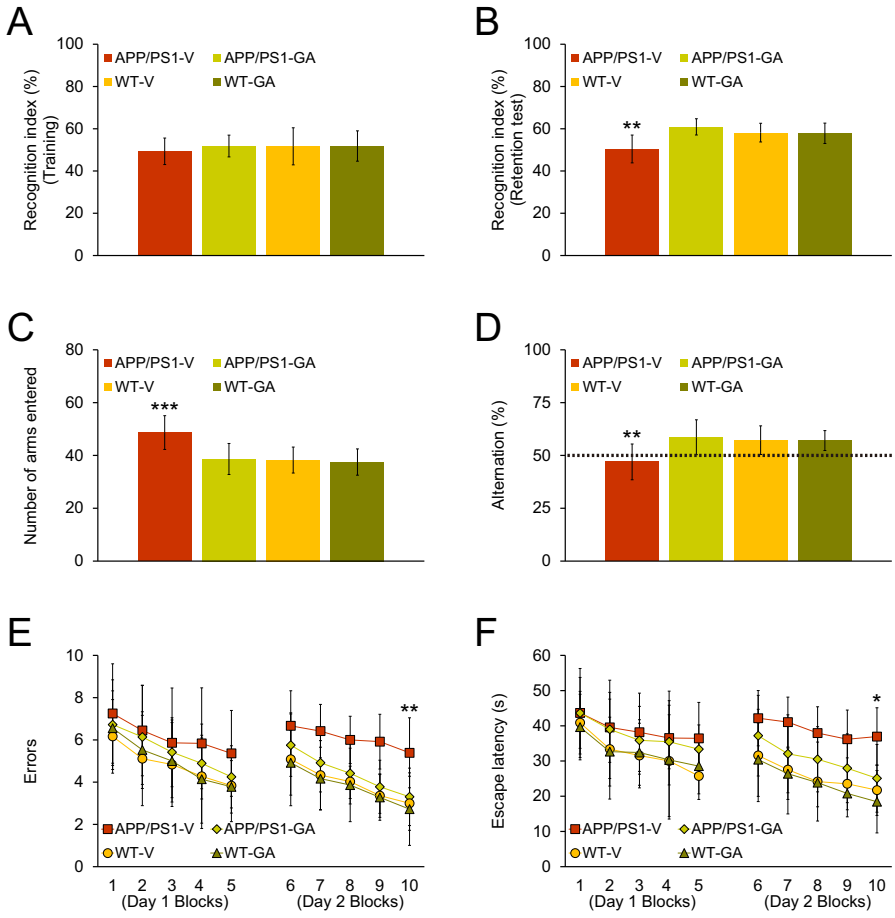

Figure 1. Oral GA therapy restores cognitive function in APP/PS1 mice. All mice were tested in a behavioral battery at 18 months of age. Recognition index (%) in the novel object recognition test is shown for training (*A*) and retention (*B*) phases. Y-maze test data are represented as total arm entries (*C*) and spontaneous alternation (*D*). Two-day radial arm water maze test data are shown with five blocks per day for errors (*E*) and for escape latency (*F*). Data were obtained from APP/PS1 mice treated with vehicle (*APP/PS1-V*, $n = 12$) or GA (*APP/PS1-GA*, $n = 12$), and WT littermates that were treated with vehicle (*WT-V*, $n = 12$) or GA (*WT-GA*, $n = 12$) for 6 months after baseline behavioral testing at 12 months of age. Data for *A-F* are presented as mean ± S.D. Statistical comparisons for *A-F* are between-groups. *, $p < 0.05$; **, $p < 0.01$; ***, $p < 0.001$ for APP/PS1-V *versus* the other treated mice.

Adding to brain parenchymal deposition of β-amyloid as senile plaques, 83% of AD patients manifest cerebral vascular β-amyloid deposits known as cerebral amyloid angiopathy (CAA) (29). In this regard, we blindly counted Aβ antibody (4G8)-stained cerebral vascular β-amyloid deposits in walls of penetrating arteries at the pial surface in RSC and EC regions, and in small arteries at the hippocampal fissure and brachium of the superior colliculus in the hippocampal area. APP/PS1 mice that received GA had significant reductions in mean numbers of CAA deposits in all three brain regions examined (20–29%; Fig. 3, *A* and *B*; *, $p < 0.05$; **, $p < 0.01$; ***, $p < 0.001$).

We moved on to validate histological results with biochemical analysis of Aβ species in brain homogenates by sandwich ELISA. In the TBS-soluble fraction, GA-treated APP/PS1 mice had significantly decreased $A\beta_{1\text{-}40}$ (38%) and $A\beta_{1\text{-}42}$ (54%) compared with vehicle-treated APP/PS1 mice (Fig. 3*C*; **, $p <$ 0.01 for $A\beta_{1\text{-}40}$ and ***, $p \leq 0.001$ for $A\beta_{1\text{-}42}$). A similar pattern of GA reductions was noted when considering the detergent-soluble fraction for $A\beta_{1\text{-}40}$ (33%) and $A\beta_{1\text{-}42}$ (43%) (Fig. 3*D*; **, $p \leq 0.01$ for $A\beta_{1\text{-}40}$ and ***, $p < 0.001$ for $A\beta_{1\text{-}42}$). The guanidine-HCl–soluble pellet, which most closely reflects β-amyloid deposits, disclosed GA-dependent reductions in APP/PS1 brain homogenates for $A\beta_{1\text{-}40}$ (35%) and $A\beta_{1\text{-}42}$ (34%) (Fig. 3*E*; ***, $p \leq 0.001$ for $A\beta_{1\text{-}40}$ and **, $p < 0.01$ for $A\beta_{1\text{-}42}$).

Oral GA therapy has dual effects on α- and β-secretases

Mitigation of cerebral amyloid pathology by long-term GA oral treatment could be owed to 1) shifting equilibrium toward brain-to-blood Aβ efflux (30), 2) decreasing expression of *APP* or *PS1* transgenes, or 3) modulating APP cleavage. To begin addressing these possibilities, we assayed plasma $A\beta_{1\text{-}40}$ and $A\beta_{1\text{-}42}$ species in peripheral blood samples from each APP/PS1 mouse group, but did not detect between-groups differences (data not shown). We then compared transgene-derived APP or PS1 proteins in brain homogenates from GA- and vehicle-treated APP/PS1 mice by Western blotting, and found similar band densities between-groups, showing that long-term GA oral therapy does not alter transgene-derived APP (Fig. 4*A*) or PS1 (data not shown) proteins.

Having ruled out the first two possibilities, we moved on to assess APP metabolites, including nonamyloidogenic soluble APP-α (sAPP-α), amyloidogenic soluble APP-β (sAPP-β), β-C-terminal APP fragment (β-CTF/C99), phospho-β-CTF (P-β-CTF/P-C99), and Aβ species. Although holo-APP protein

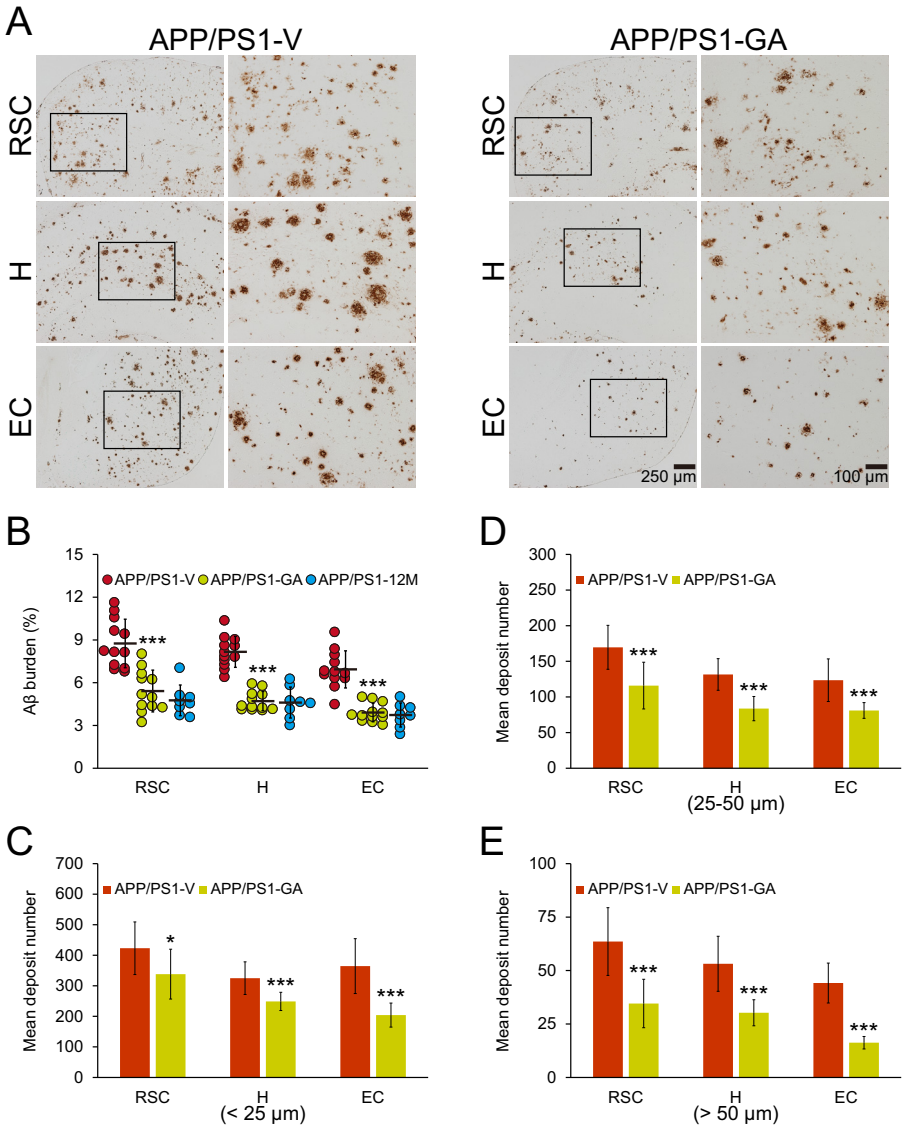

Figure 2. Attenuated cerebral amyloidosis in APP/PS1 mice after oral GA therapy. Representative images were obtained from vehicle- (*APP/PS1-V*) or GA- (*APP/PS1-GA*) treated APP/PS1 mice for 6 months starting at 12 months of age (mouse age at sacrifice = 18 months). *A*, immunohistochemistry using an $A\beta_{17\text{-}24}$ mAb (*4G8*) highlights cerebral β-amyloid deposits as amber signals. Brain regions shown include the RSC (*top*), H (*middle*), and EC (*bottom*). Each image at *right* is a higher magnification image from *insets*. *B*, quantitative image analysis is shown for Aβ burden from brain sections stained with $A\beta_{17\text{-}24}$ mAb (*4G8*). *C–E*, morphometric analysis of cerebral parenchymal β-amyloid deposits. Mean plaque size is shown on the *y axis* based on blind assignment to one of three mutually exclusive categories: small (<25 μm, *C*), medium (between 25 and 50 μm, *D*), or large (>50 μm, *E*). *B-E*, brain region is shown on the *x axis* (*RSC*, *H*, and *EC*). Twelve-month–old untreated APP/PS1 mice (*APP/PS1-12M, n* = 8) were included in *B* as a baseline control. Data for *B-E* are presented as mean ± S.D. Statistical comparisons for *B-E* are between-groups within each brain region. *, $p < 0.05$; ***, $p < 0.001$ for APP/PS1-GA *versus* APP/PS1-V mice (*B-E*) or 12-month-old untreated APP/PS1 mice (*B*).

was comparable between-groups, densitometry disclosed significantly elevated nonamyloidogenic APP processing to sAPP-α in brain homogenates from GA- *versus* vehicle-treated APP/PS1 mice (Fig. 4, *A* and *B*; ***, $p < 0.001$). By contrast, amyloidogenic APP processing to sAPP-β as well as C99 and P-C99 was significantly reduced in brain homogenates from GA-treated APP/PS1 mice (Fig. 4, *A* and *C*, and *D*; ***, $p < 0.001$). Additionally, band densities of 4-kDa monomers (Fig. 4*A*) and species between 25 and 75 kDa (putative Aβ oligomers) were also decreased in brain homogenates from GA-treated APP/PS1 mice compared with vehicle-treated animals (Fig. 4*A*). We corroborated this by 82E1 sandwich ELISA for Aβ oligomers (Fig. 4*E*; **, $p < 0.01$ for APP/PS1-GA *versus* APP/PS1-V mice).

Collectively, our biochemical results suggest that GA therapy exerts dual activities on elevating nonamyloidogenic and reducing amyloidogenic APP processing. We moved on to examine a disintegrin and metalloproteinase domain-containing protein 10 (ADAM10, an α-secretase candidate) and β-site APP cleaving enzyme 1 (BACE1, β-secretase) proteins in brain homogenates from each group of APP/PS1 mice by Western blotting. Both precursor ADAM10 (pADAM10, 90-kDa band) and mature (active) ADAM10 (mADAM10, 68-kDa band) protein expressions were significantly increased in brain homogenates from GA-treated mice (Fig. 5, *A–C*; ***, $p < 0.001$ for pADAM10 and mADAM10). ADAM10 is regulated by the proprotein convertase, furin, which activates the enzyme by cleaving the zymogen

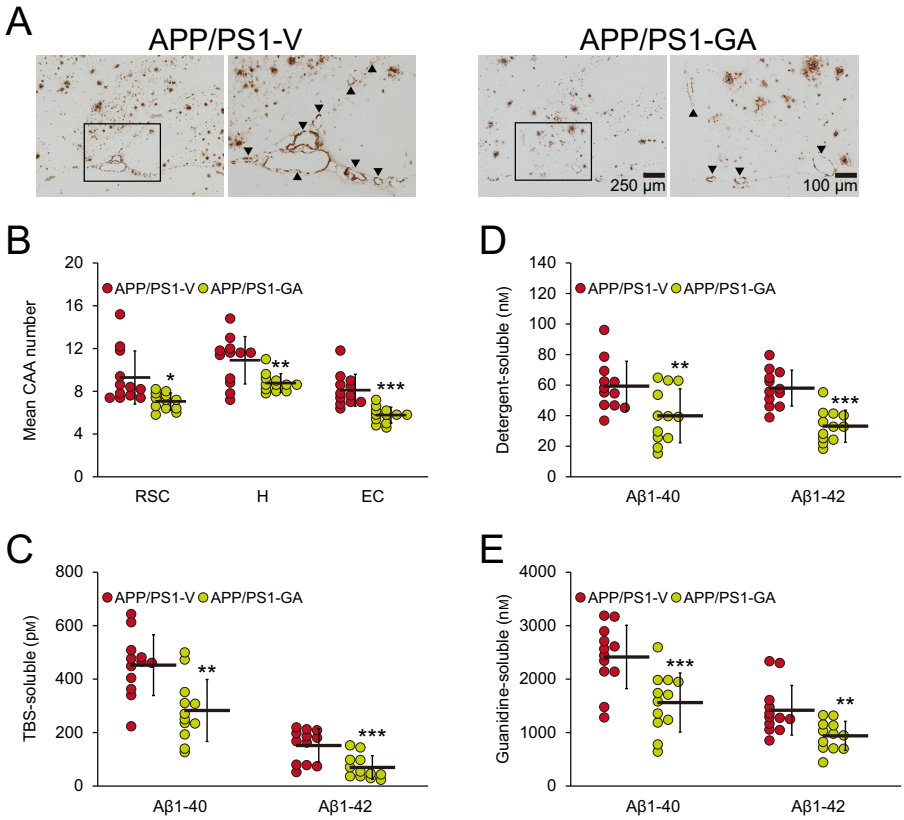

Figure 3. GA therapy decreases cerebral vascular β-amyloid deposits and Aβ abundance. Representative images were obtained from vehicle- (*APP/PS1-V*) or GA- (*APP/PS1-GA*) treated APP/PS1 mice for 6 months starting at 12 months of age (mouse age at sacrifice = 18 months). *A*, immunohistochemistry using an $A\beta_{17-24}$ mAb (*4G8*) highlights cerebral amyloid angiopathy as amber signals at the hippocampal fissure in the hippocampal area. Each image at *right* is a higher magnification image from *insets*. *B*, severity of cerebral amyloid angiopathy (mean numbers of CAA deposits per mouse) is shown on the *y axis*, and brain region is shown on the *x axis* (*RSC*, *H*, and *EC*). *C–E*, brain homogenates from TBS-soluble (*C*), detergent-soluble (*D*), or 5 M guanidine HCl-extractable (*E*) fractions were individually measured by sandwich ELISA for human $A\beta_{1-40}$ and $A\beta_{1-42}$. *B–E*, data were obtained from APP/PS1 mice treated with vehicle (*APP/PS1-V*, $n = 12$) or GA (*APP/PS1-GA*, $n = 12$) for 6 months beginning at 12 months of age (mouse age at sacrifice = 18 months). Data for *B–E* are presented as mean ± S.D. Statistical comparisons for *B* are between-groups within each brain region, and for *C–E* are between-groups for each Aβ species. *, $p < 0.05$; **, $p < 0.01$; ***, $p \leq 0.001$ or $p < 0.001$ for APP/PS1-GA *versus* APP/PS1-V mice (*B–E*).

into the mature form (31). Therefore, we investigated furin expression in brain homogenates from each group of APP/PS1 mice by Western blotting. Results showed that furin protein abundance was significantly increased in brains from GA- compared with vehicle-treated mice (Fig. 5, *A* and *D*; ***, $p < 0.001$). By contrast, BACE1 protein expression was reduced in brain homogenates from GA- *versus* vehicle-treated APP/PS1 mice (Fig. 5, *A* and *E*; **, $p < 0.01$, APP/PS1-GA compared with APP/PS1-V mice). To assess if GA altered transcription of *Adam10* or *Bace1* in the brain, we assayed both mRNA species by quantitative real-time PCR (q-PCR). We did not observe any between-groups differences (Fig. 6, *A* and *B*), suggesting that GA functions at the post-transcriptional level.

To test whether GA therapy impacted secretase activity, we assayed α- and β-secretase enzymatic kinetics in brain homogenates from APP/PS1-GA *versus* APP/PS1-V mice. Repeated-measures ANOVA showed that α-secretase activity kinetics were significantly accelerated, although kinetics for β-secretase activity were reduced in brain homogenates from GA- *versus* vehicle-treated APP/PS1 mice (Fig. 6, *C* and *D*; ***, $p < 0.001$). Therefore, GA therapy exerts dual effects on α- and β-secretases by modulating protein levels and enzymatic activity of both secretases.

To assess whether GA directly inhibited β-secretase, we assayed GA dose-response in a cell-free β-secretase activity inhibitor assay. The result was positive, as GA dose-dependently inhibited β-secretase enzymatic activity, with statistical significance at the 6.25 and 12.5 μM doses (Fig. 6*E*; *, $p < 0.05$). These results support that GA therapy up-regulates α-secretase and down-regulates β-secretase activity, with a net positive shift toward nonamyloidogenic APP processing.

GA attenuates neuroinflammation and oxidative stress in APP/PS1 brains

GA reportedly has anti-inflammatory and anti-oxidant properties (9, 12, 13). Therefore, we examined putative effects of GA on neuroinflammatory processes and oxidative stress in APP/PS1 brains. We began this line of investigation by elucidating cerebral β-amyloid deposit-associated gliosis (*i.e.* astrocytosis and microgliosis) by quantitative immunohistochemical analyses. APP/PS1-V mice exhibited hyperplasia and hypertrophy of β-amyloid plaque-associated reactive astrocytes and microglia. We observed positive immunostaining for the astrocytic activation marker, glial fibrillary acidic protein (GFAP), and the structural marker of activated microglia, ionized calcium-binding adapter molecule 1 (Iba1), in glial somata and processes.

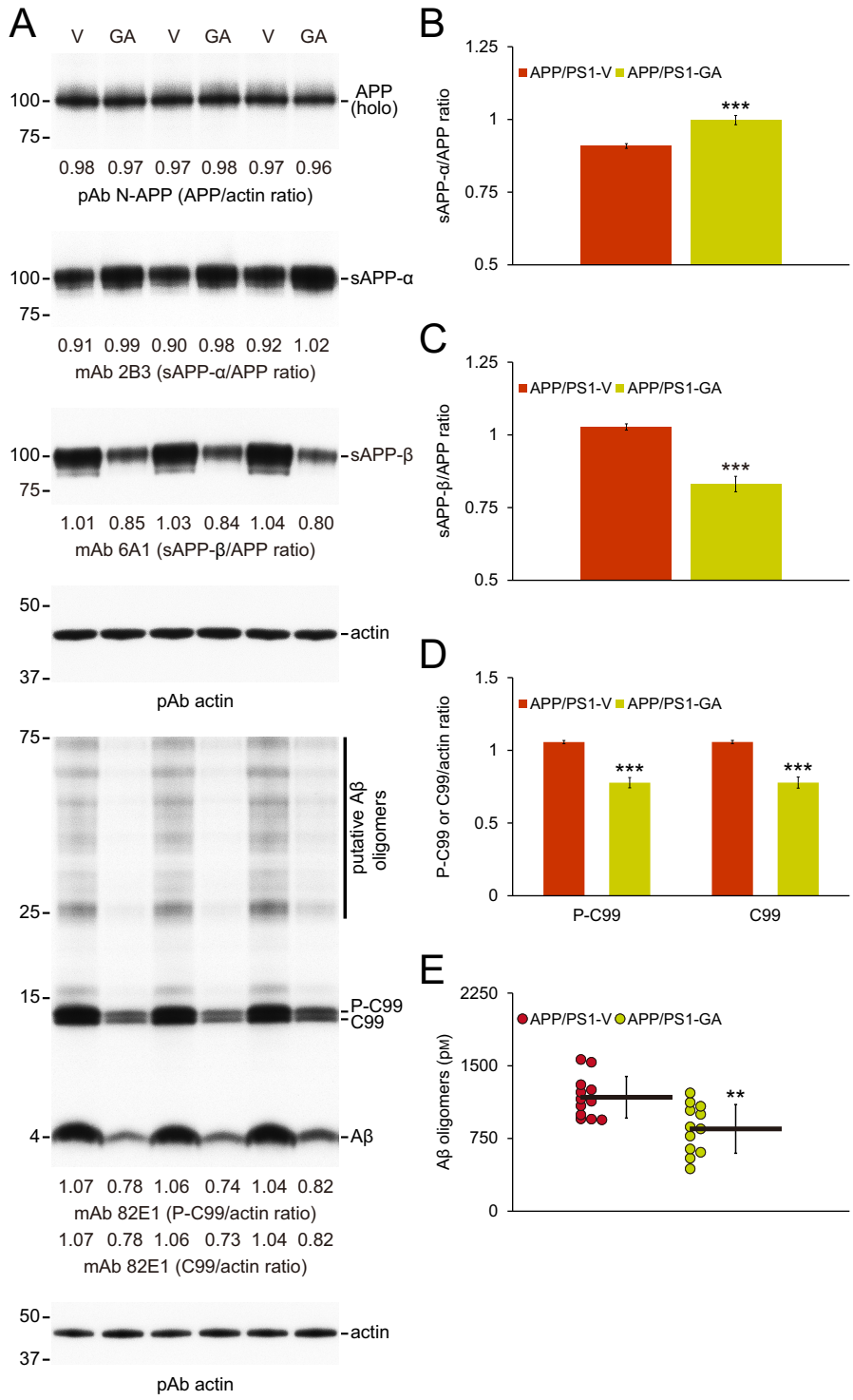

Figure 4. GA therapy promotes nonamyloidogenic and inhibits amyloidogenic APP processing. *A*, Western blots are shown using N-terminal APP pAb (*N-APP*), C-terminal sAPP-α mAb (*2B3*), or C-terminal anti-sAPP-β-sw mAb (*6A1*). We also used N-terminal amyloid-$\beta_{1\text{-}17}$ mAb (*82E1*), which detects amyloidogenic APP cleavage fragments, including Aβ monomers and oligomers as well as phospho-C99 (*P-C99*) and nonphospho-C99 (*C99*). Actin is included as an internal reference control. Densitometry results are shown for ratios of sAPP-α or sAPP-β to APP (*B* and *C*) and for P-C99 or C99 to actin (*D*). *E*, abundance of Aβ oligomers in detergent-soluble brain homogenates (measured by sandwich ELISA) is shown. Data were obtained from APP/PS1 mice treated with vehicle (*APP/PS1-V*, $n = 12$) or GA (*APP/PS1-GA*, $n = 12$) for 6 months starting at 12 months of age. Data for *B-E* are presented as mean ± S.D. Statistical comparisons for *B*, *C* and *E* are between-groups, and for *D*, between-groups for each protein. **, $p < 0.01$; ***, $p < 0.001$ for APP/PS1-GA *versus* APP/PS1-V mice.

Numerous minute GFAP-positive astrocytic processes were distributed between neurons, and GFAP expression was co-localized with dystrophic neurites near β-amyloid deposits (Fig. 7*A*). By contrast, long-term GA-treated APP/PS1 mice had decreased numbers of reactive astrocytes and microglia (Fig. 7*A*), and quantitative data disclosed that GA therapy

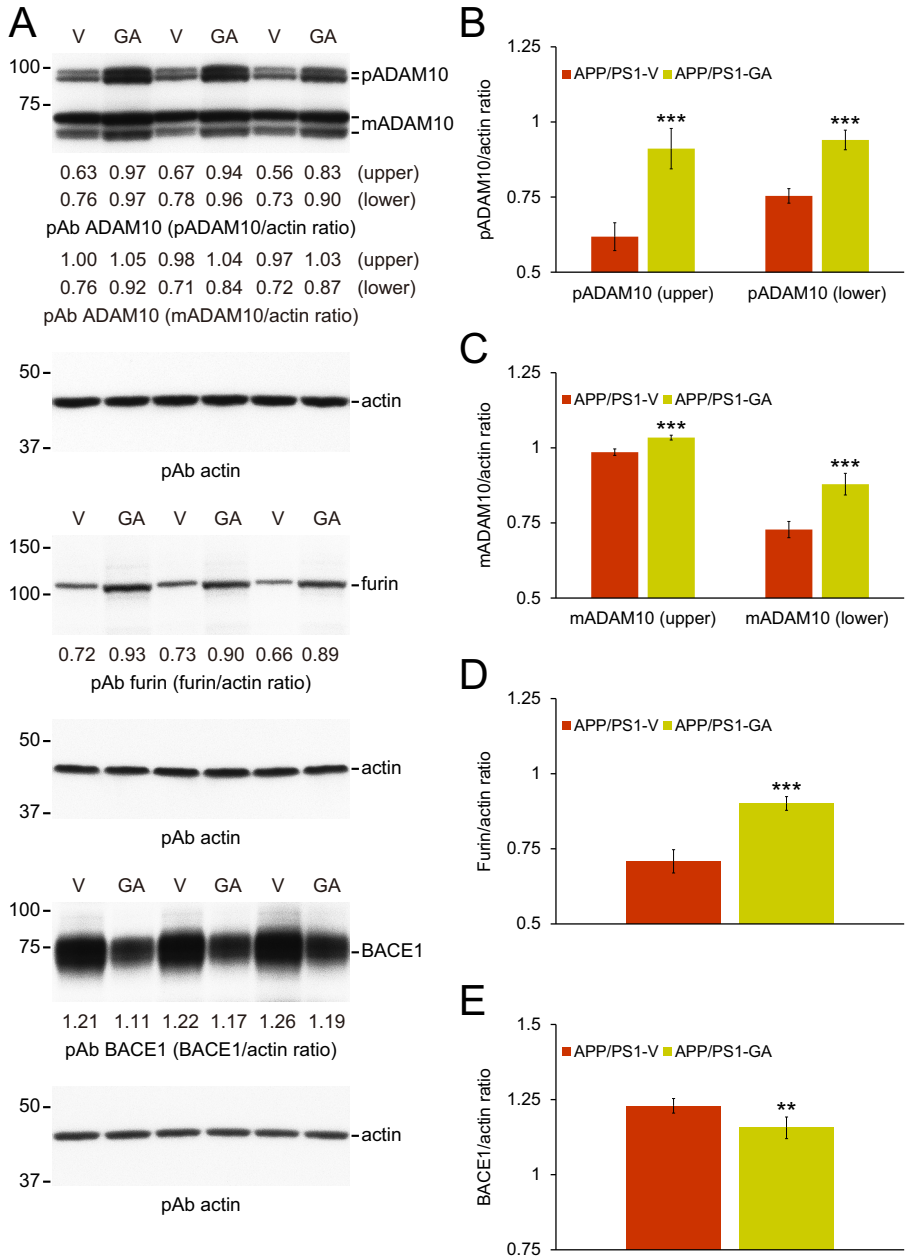

Figure 5. GA increases ADAM10 and decreases BACE1 proteins, and elevates abundance of the ADAM10 activating enzyme furin in APP/PS1 brains. *A*, Western blots are shown using C-terminal ADAM10 pAb (*ADAM10*), C-terminal BACE1 pAb (*BACE1*), or furin pAb (*furin*). Actin is included as an internal loading control, and densitometry results are shown for ratios of precursor ADAM10 (*pADAM10*) or mature ADAM10 (*mADAM10*) to actin (*B* and *C*), for furin to actin (*D*), or for BACE1 to actin (*E*). Data for *A-E* were obtained from APP/PS1 mice that received vehicle (*APP/PS1-V*, $n = 12$) or GA (*APP/PS1-GA*, $n = 12$) for 6 months commencing at 12 months of age. Data for *B-E* are presented as mean ± S.D. Statistical comparisons for *B-E* are between-groups for each protein. **, $p < 0.01$; ***, $p < 0.001$ for APP/PS1-GA *versus* APP/PS1-V mice.

significantly attenuated both forms of reactive gliosis (Fig. 7, *B* and *C*; **, $p < 0.01$; ***, $p < 0.001$). These effects were sex-independent (data not shown).

We also investigated protein expression of two key brain oxidative stress markers: superoxide dismutase 1 (SOD1) and GSH peroxidase 1 (GPx1). Western blots of brain homogenates from GA-treated APP/PS1 mice showed that both SOD1 and GPx1 proteins were decreased compared with APP/PS1-V brains (Fig. 8*A*), and densitometry confirmed statistically significant reductions (Fig. 8, *B* and *C*; ***, $p < 0.001$). Amelioration of oxidative stress was complete, because abundance of either protein did not significantly differ from either WT mouse group ($p > 0.05$). These effects were sex-independent (data not shown). Collectively, these data suggest that 6-month oral GA therapy alleviates neuroinflammation and stabilizes oxidative stress in APP/PS1 brains.

Discussion

As natural dietary compounds present throughout evolution, nutraceuticals are well-tolerated, either alone or in combination with other therapies. GA is a plant-derived nutraceutical

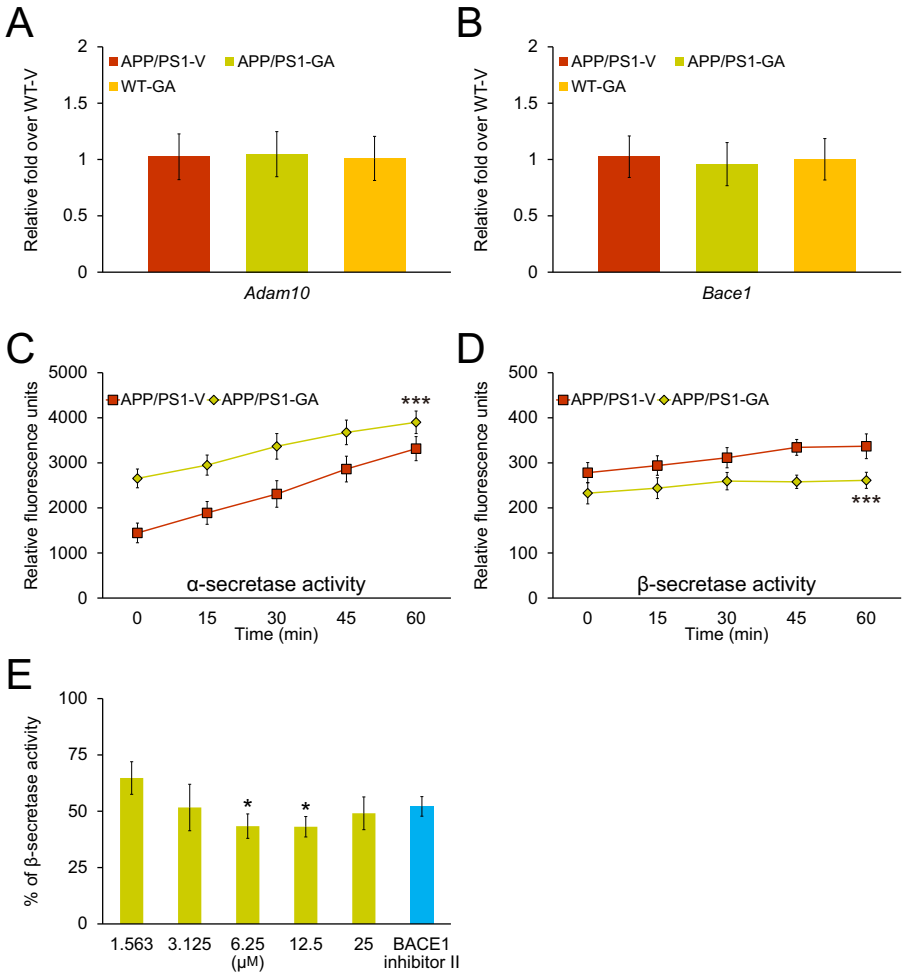

Figure 6. GA therapy modulates α- and β-secretase activities in brains from APP/PS1 mice. *A* and *B*, there are no between-groups differences on *Adam10* or *Bace1* mRNA expression in APP/PS1 brains after GA treatment. Data are expressed as relative-fold over WT-V mice. Data for *A* and *B* were obtained from APP/PS1 mice that received vehicle (*APP/PS1-V*, $n = 12$) or GA (*APP/PS1-GA*, $n = 12$) for 6 months commencing at 12 months of age. WT mice treated with vehicle (*WT-V*, $n = 12$) or with GA (*WT-GA*, $n = 12$) were also included as controls. *C* and *D*, α- and β-secretase activity assay results are shown. Relative fluorescence units are shown on the *y* axis, and reaction time is represented on the *x* axis. Cell-free β-secretase inhibitor activity assay results are shown (*E*). Results are expressed as % of β-secretase inhibitor activity on the *y* axis relative to 100% initial activity of β-secretase in the absence of GA. Data for *A* and *B* were obtained from APP/PS1 mice that received vehicle (*APP/PS1-V*, $n = 12$) or GA (*APP/PS1-GA*, $n = 12$) for 6 months commencing at 12 months of age. Data for *C* and *D* are presented as mean ± S.D. Statistical comparisons for *A* and *B* are between-groups. Statistical comparisons for *E* are between-doses. ***, $p < 0.001$ for APP/PS1-GA *versus* APP/PS1-V mice. *, $p < 0.05$ for 6.25 or 12.5 μM *versus* 1.563 μM and similar results were observed in 2 to 3 independent experiments.

that has anti-inflammatory and anti-oxidant properties (11), and we were specifically interested in GA because this moiety is present in other nutraceuticals that we have shown to be therapeutic in preclinical AD model mice (2–5). We therefore tested if administering oral GA therapy from 6 to 12 months of age to APP/PS1 mice modified cognitive function and AD-like pathology. Results showed complete mitigation of impaired learning and memory, reduced cerebral amyloidosis, and attenuated neuroinflammation and oxidative stress. These beneficial effects occurred with increased ADAM10 and reduced BACE1 protein abundance and enzymatic activity, beneficially shifting the balance toward nonamyloidogenic APP metabolism. When taken together, these results provide preclinical evidence supporting oral GA therapy as an AD prophylaxis.

According to the Registry of Toxic Effects of Chemical Substances (RTECS), the GA acute intraperitoneal lethal dose for 50% survival (LD_{50}) is 4,300 mg/kg in the mouse. The no observed adverse effect level (NOAEL) for mouse oral GA is 5,000 mg/kg (32). Tolerable daily intake for humans can be extrapolated from rodent NOAEL threshold data by dividing the NOAEL by the uncertainty factor (*i.e.* interspecies and individual variation) (33, 34). Assuming a default uncertainty factor of 100 (34), the 5,000 mg/kg mouse NOAEL yields human tolerable daily intake for GA of 50 mg/kg, or 3,000 mg for a 60-kg person. In the present study, we orally administered 20 mg/kg/day to mice. To extrapolate this mouse dose to humans, we multiply 20 mg/kg by the mouse factor of 3, and then divide by the human factor of 37 (35). This calculation results in a GA human equivalent dose of 1.622 mg/kg, which equates to 97.32 mg of GA for a 60-kg person. The dose we gave to mice is orders of magnitude below tolerable levels, and there was no morbidity or mortality observed in this study. Furthermore, we did not observe pathological findings in any major organs at autopsy, including the skin, hair, brain, eyes, ears, lung, heart, liver, digestive tract, or kidneys. Even so, it remains possible that long-term up-regulation of ADAM10 and/or down-regulation of

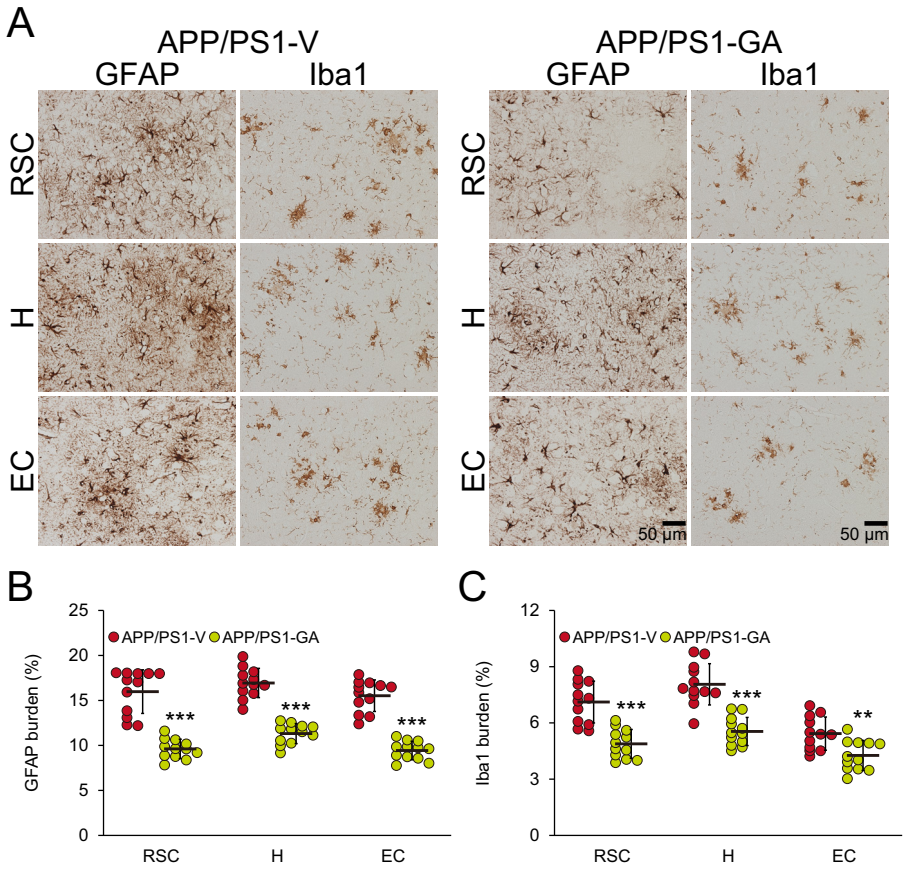

Figure 7. Reduced gliosis in APP/PS1-GA brains after GA treatment. *A*, representative images were captured from APP/PS1 mice treated with vehicle (*APP/PS1-V*) or GA (*APP/PS1-GA*) for 6 months starting at 12 months of age (mouse age at sacrifice = 18 months). Immunohistochemistry for GFAP and Iba1 shows β-amyloid deposit-associated astrocytosis (*left*) and microgliosis (*right*) for each group. Brain regions shown include: RSC (*top*), H (*middle*), and EC (*bottom*). Quantitative image analysis for astrocytosis (*B*) or microgliosis (*C*) burden is shown. Brain regions are shown on the *x* axis. Data for *B* and *C* are presented as mean ± S.D. Statistical comparisons for *B* and *C* are within each brain region and between-groups. **, $p < 0.01$; ***, $p < 0.001$ for APP/PS1-GA *versus* APP/PS1-V mice.

BACE1 might lead to unwanted side effects. Therefore, investigating the toxicity profile of long-term GA treatment in humans is warranted.

In terms of bioavailability, GA oral administration produces maximum absorption at 60 min for rodents (36) and 87 min for humans (37). A dual mechanism has been suggested for gastric absorption of GA: rapid for intact GA and slow for conjugated derivatives (*i.e.* 4-*O*-methylgallic acid) (38). GA has low molecular weight and has been shown to cross the blood-brain-barrier in rodents (39).

Three proteases, known as α-, β-, and γ-secretases, are responsible for APP processing. In the amyloidogenic pathway, APP is internalized into endocytic compartments and cleaved by β- and γ-secretases to generate Aβ species ($A\beta_{40}$ and $A\beta_{42}$), which then form oligomeric and multimeric aggregates that are neurotoxic (40–43). Interestingly, newly generated Aβ species enter into systemic equilibrium between soluble and deposited forms (40). On the other hand, α-secretase APP processing is the homeostatic Aβ lowering pathway. In this nonamyloidogenic pathway, APP is proteolyzed by α-secretase at the cell membrane. The α-secretase cleavage event within the Aβ domain: 1) precludes Aβ generation and 2) liberates secreted sAPP-α and membrane-bound α-CTF/C83 (41, 44).

Aβ lowering strategies, including secretase targeting, have become essential therapeutic approaches in AD. In this report, we show that GA therapy exerts beneficial effects on ameliorating cerebral amyloid pathology (including parenchymal and cerebral vascular β-amyloid deposits), concomitant with decreasing Aβ species. We show that nonamyloidogenic sAPP-α protein expression is significantly increased in brain homogenates from GA-treated APP/PS1 mice; whereas amyloidogenic sAPP-β and β-CTFs (*i.e.* C99 and P-C99) are significantly decreased. These data suggest that GA dually impacts both amyloidogenic and nonamyloidogenic pathways, with a net positive effect of shifting the balance toward reducing Aβ production.

In this report, we show that GA is a dual modulator of α/β-secretase activity. Specifically, our data support that GA enhances ADAM10 and inhibits BACE1 activity to promote nonamyloidogenic APP processing. Importantly, GA did not alter brain transcription of *Adam10* and *Bace1*, suggesting a post-transcriptional mode of action. Because GA therapy significantly elevated mature (active) ADAM10 in APP/PS1 brains, we hypothesized a post-translational mechanism. ADAM10 is produced in an inactive form, and the proprotein convertase, furin, cleaves the ADAM10 zymogen to activate it (31). In this regard, we show increased protein expression of furin in brain homogenates from GA-treated mice. Increased brain furin

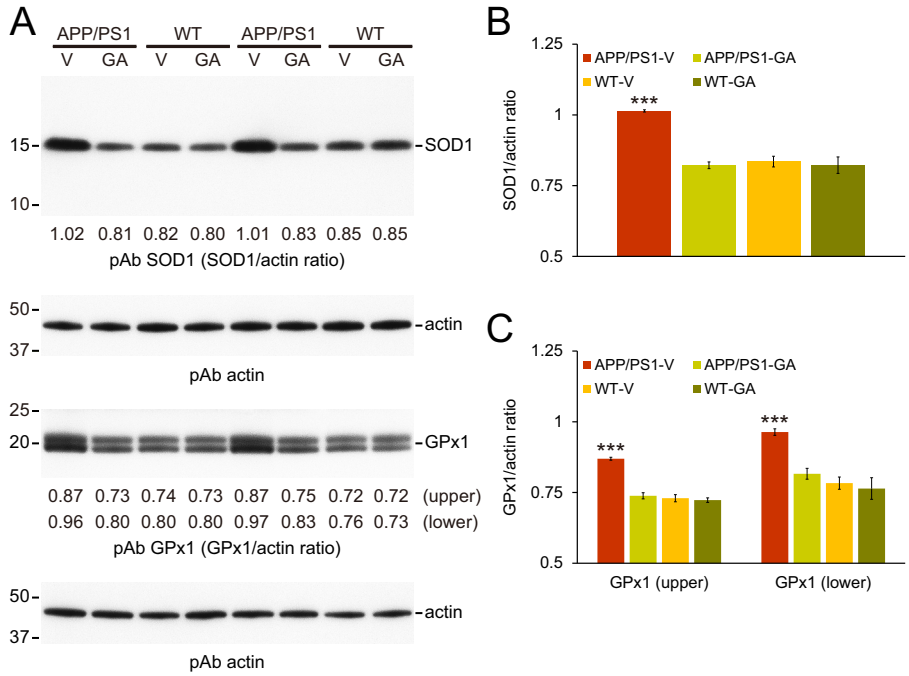

Figure 8. GA therapy stabilizes brain oxidative stress in APP/PS1 mice. *A*, Western blots are shown using anti-Cu/Zn SOD pAb (*SOD1*) or anti-GPx1 pAb (*GPx1*), with actin as an internal loading control. Densitometry data are shown below each lane for SOD1 (*B*) or GPx1 (two bands; *upper* and *lower*) as ratios to actin (*C*). Data for *B* and *C* were obtained from APP/PS1 mice treated with vehicle (*APP/PS1-V*, $n = 12$) or GA (*APP/PS1-GA*, $n = 12$), and also for WT littermates that received vehicle (*WT-V*, $n = 12$) or GA (*WT-GA*, $n = 12$) for 6 months commencing at 12 months of age (mouse age at sacrifice = 18 months). Data for *B* and *C* are presented as mean ± S.D. Statistical comparisons for *B* and *C* are between-groups for each band. ***, $p < 0.001$ for APP/PS1-V *versus* the other treated mice.

abundance is associated with elevated mADAM10. Unexpectedly, pADAM10 is also increased in the brain following GA therapy. We previously observed increases in both forms of ADAM10 after EGCG treatment (3), and a similar positive feedback loop may exist with GA, whereby ADAM10 cleavage promotes pADAM10 protein expression. Furthermore, we conducted experiments in a cell-free β-secretase activity assay and found that GA directly inhibits BACE1 enzymatic activity post-translationally.

We further show that elevation of active ADAM10 correlates with increased α-secretase APP cleavage and sAPP-α protein abundance in APP/PS1 brains. The sAPP-α generated by α-secretase APP cleavage has both neurotrophic and neuroprotective properties (45, 46) and has been shown to enhance long-term potentiation (47). Interestingly, our previous study showed that sAPP-α is capable of inhibiting BACE1 though physical interactions (48). In support, others have shown that sAPP-α can autoregulate APP metabolism (49–51). Therefore, it remains possible that GA promotion of α-secretase could indirectly inhibit β-secretase activity.

Although there is evidence linking cognitive decline with cerebral amyloid pathology in AD patients (52, 53), a subset of elderly without cognitive impairment have striking AD pathology, including "senile" plaques and/or neurofibrillary tangles (54, 55). When considering preclinical mouse models of AD, accumulating evidence has shown that improved cognitive function occurs in parallel with mitigation of cerebral amyloid pathology in a subset of studies (4, 23–27, 56–59), whereas others have pointed out de-coupling of cognitive function from AD-like pathology (60, 61). This discrepancy has led to an alternate hypothesis that soluble, oligomeric forms of Aβ might impair cognition due to synaptotoxicity and neurotoxicity (62–65). Supporting this, a positive link has been reported between increased Aβ oligomer levels and behavioral impairment in rodent models (57, 61). Accordingly, we show that Aβ oligomers are significantly decreased after oral GA therapy.

Shifting from protective to destructive functions of glial cells may contribute to neurotoxicity and synaptotoxicity in neurodegenerative diseases. In the AD brain, reactive gliosis co-exists in temporal and spatial proximity to β-amyloid plaques, and diffuse β-amyloid deposits attract and activate cytokine-secreting microglia, which can in turn activate astrocytes that cooperatively produce cytokines. This self-propagating "cytokine cycle" promotes further release of acute-phase reactants, proinflammatory cytokines, and immunostimulatory molecules, leading to generation of reactive oxygen species that are toxic at supraphysiologic levels. These proinflammatory substances in turn further enhance inflammatory responses and likely bystander neuronal damage in the AD brain (66–69). Our understanding of the role that neuroinflammatory processes play in AD progression is becoming clearer. Although there is consensus that glial cells ultimately fail to clear β-amyloid deposits (23, 66–72), it is now appreciated that not all forms of gliosis are deleterious, and this is underscored by well-documented dichotomous roles of microglia and astrocytes in exacerbating or mitigating AD pathology depending on context (67–69).

Here, we show that oral GA therapy dampens β-amyloid plaque-associated microgliosis and astrocytosis. One possibility is that GA exerts anti-inflammatory effects that are independent

of Aβ lowering. However, neuroinflammation and cerebral amyloidosis generally correlate in human AD and in mouse models, making it complex if not impossible to tease them apart *in vivo*.

Anti-oxidants are essential biomolecules that protect the body against the hazardous effects of oxidative stress and imbalanced redox homeostasis (73). Most oxidative stress occurs in the form of intracellular superoxide anions, singlet oxygen, hydrogen peroxide, and other reactive oxygen species that are generated in mitochondria, the cellular organelle responsible for a diverse array of functions such as metabolism, ATP synthesis, Ca^{2+} signaling, cell survival, and growth (74). Oxidative stress has been implicated in AD etiology (75, 76), and GA is a potent anti-oxidant because of its free radical scavenging properties. For example, GA has electron-donating sites on the benzene ring (*i.e.* 3-, 4-, and 5-hydroxyl) yielding phenoxyl radical resonance structures conferring stability to this intermediate or even terminating free radical chain reactions altogether. Additionally, GA has a carboxylic acid group that can act as a lipid anchor to protect against lipid peroxidation. Indeed, we show that GA therapy completely stabilizes brain expression of SOD1 and GPx1 to baseline levels in APP/PS1 mice, which did not differ from nontransgenic littermates.

In conclusion, we report that administering 6-month oral GA therapy to the APP/PS1 mouse model of cerebral amyloidosis completely remediates behavioral deficits, ameliorates cerebral amyloidosis, and reduces Aβ abundance. GA treatment further alleviates neuroinflammation and stabilizes oxidative stress. If the APP/PS1 mouse model reflects the clinical syndrome, then dietary supplementation with GA represents a viable therapeutic modality for AD.

Experimental procedures

Ethics statement

All experiments were performed in accordance with the guidelines of the National Institutes of Health, and all animal studies were approved by the Saitama Medical University Institutional Animal Care and Use Committee. Mice were humanely cared for during all experiments, and all efforts were made to minimize suffering.

Mice

Male B6.Cg-Tg(APP_{swe}, PSEN1dE9)85Dbo/Mmjax mice (bearing "Swedish" $APP_{K595N/M596L}$ and *PS1* exon 9-deleted mutant human transgenes) on the congenic C57BL/6J background (designated APP/PS1 mice) (77) and female C57BL/6J mice were obtained from The Jackson Laboratory (Bar Harbor, ME, USA). For colony maintenance, male APP/PS1 mice were bred with female C57BL/6J mice to yield APP/PS1 and WT offspring, so all experimental APP/PS1 mice and WT littermates in this study are on the C57BL/6J background.

GA was obtained from Sigma-Aldrich. Twenty mg of GA was resuspended in 25 μl of 100% DMSO and then diluted with distilled water to a final concentration of 0.2% DMSO. The regent was freshly prepared daily prior to each treatment. We randomly assigned APP/PS1 mice to two treatment groups (n = 12 per condition; six per sex): GA (APP/PS1-GA) or vehicle (distilled water containing DMSO at a final concentration of 0.2%; APP/PS1-V). Additionally, WT littermates received the same two treatments (n = 12 per group; six of each sex) as follows: WT-GA or vehicle (WT-V). To determine whether treatment prevented *versus* reversed kinetics of cerebral amyloid accumulation, we included eight untreated APP/PS1 mice at 12 months of age (APP/PS1-12M mice, four of each sex) for analysis of β-amyloid pathology. After baseline behavioral assessment just prior to dosing (at 12 months of age), animals were orally treated (via gavage using a 6202 gastric tube with a rounded silicone-coated tip, Fuchigami Kikai, Kyoto, Japan) with GA (20 mg/kg) or vehicle once daily for 6 months. Mice were housed in a specific pathogen-free barrier facility with a 12/12-h light/dark cycle and *ad libitum* access to food and water.

Behavioral analyses

To assess episodic memory, mice were habituated in a cage for 4 h, and two objects of different shapes were concurrently provided for 10 min. The number of times that the animal explored the familiar object (defined as number of instances where an animal directed its nose 2 cm or less from the object) was counted for the initial 5 min of exposure (training phase). To test memory retention on the following day, one of the familiar objects was replaced with a different-shaped novel object and explorations were recorded for 5 min (retention test). The recognition index, taken as a measurement of episodic memory, is reported as frequency (%) of explorations of the novel *versus* familiar object (78).

To measure exploratory activity and spatial working memory, mice were individually placed in one arm of a radially symmetric Y-maze made of opaque gray acrylic (arms, 40 cm long and 4 cm wide; walls, 30 cm tall), and the sequence of arm entries and total number of entries were counted over a period of 8 min, beginning when the animal first entered the central area. Percent alternation was defined as entries into sequentially different arms on consecutive occasions using the following formula: % alternation = number of alternations/(number of total arm entries – 2) × 100% (21).

To assess spatial reference learning and memory, the RAWM test was done over 2 days and consisted of triangular wedges in a circular pool (80 cm diameter) configured to form swim lanes that enclosed a central open space. Mice naïve to the task were placed in the pool and allowed to search for the platform for 60 s. Animals were dropped into a random start arm and allowed to swim until they located and climbed onto the platform (goal) over a period of 60 s. Latency to locate the platform and errors were recorded. Each mouse was given a total of 15 trials. On day 1, the goal alternated between visible and hidden, although on day 2, the goal was always hidden. All data were organized as individual blocks of three trials each. The goal arms remained in the same location for both days, whereas the start arm was randomly altered. All trials were done at the same time of day (±1 h), during the animals' light phase. To avoid interference with behavioral testing, treatment was carried out 1 h after conclusion of behavioral testing (79).

Brain tissue preparation

At 18 months of age, anesthesia was induced and maintained with isoflurane (1.5 to 2% and then 0.5%). Mice were euthanized by transcardial perfusion with ice-cold physiological saline containing heparin (10 units/ml). Brains were isolated and quartered (sagittally at the level of the longitudinal fissure of the cerebrum, and then coronally at the level of the anterior commissure). Left anterior hemispheres were weighed and snap-frozen at −80 °C for Western blotting. Left posterior hemispheres were immersed in 4% paraformaldehyde at 4 °C overnight and routinely processed in paraffin. Right anterior hemispheres were sliced into two pieces, weighed, and snap-frozen at −80 °C for α- and β-secretase activity assays. Right posterior hemispheres were sliced into two pieces. One piece including the hippocampus was weighed and snap-frozen at −80 °C for sandwich ELISA. The other piece was weighted and immersed in RNA stabilization solution (RNAlater®, Qiagen, Valencia, CA, USA) and then snap-frozen at −80 °C for q-PCR analyses.

Immunohistochemistry

Five coronal paraffin sections (per set) were cut with a 100-μm interval and 5-μm thickness spanning bregma –2.92 to –3.64 mm (80). Three sets of five sections were prepared for analyses of β-amyloid plaques, astrocytosis, and microgliosis. Primary antibodies were as follows: biotinylated anti-A$\beta_{17\text{-}24}$ mAb (1:200 dilution, 4G8; Covance Research Products, Emeryville, CA, USA), anti-GFAP pAb (1:500 dilution, Dako, Carpinteria, CA, USA), and C-terminal anti-Iba1 pAb (1:500 dilution, FUJIFILM WAKO Pure Chemical, Osaka, Japan). Immunohistochemistry was performed using a Vectastain ABC *Elite* kit (Vector Laboratories, Burlingame, CA, USA) coupled with the diaminobenzidine reaction, except that the biotinylated secondary antibody step was omitted for the biotinylated A$\beta_{17\text{-}24}$ mAb.

Image analysis

Images were acquired and quantified using SimplePCI software (Hamamatsu Photonics, Shizuoka, Japan). Images of five 5-μm sections through each anatomic ROI (*i.e.* RSC, EC, and H) were captured based on anatomical criteria (80), and we set a threshold optical density that discriminated staining from background. Selection bias was controlled for by analyzing each ROI in its entirety. For Aβ, GFAP, and Iba1 burden analyses, data are reported as the percentage of positive pixels captured divided by the full area captured. A$\beta_{17\text{-}24}$ mAb, which recognizes amino acids 18-22 (VFFAE), was used for conventional Aβ burden analysis.

For β-amyloid plaque morphometric analysis, diameters (maximum lengths) of β-amyloid plaques were blindly measured and assigned to one of three mutually exclusive plaque size categories (<25, between 25 and 50, or >50 μm). For quantitative analysis of CAA, numbers of Aβ antibody-positive cerebral vessels were blindly counted in each ROI.

ELISA

Brain A$\beta_{1\text{-}40}$ and A$\beta_{1\text{-}42}$ species were detected by a three-step extraction protocol with modifications (81). Brains were homogenized using TissueLyser LT (Qiagen) in TBS (TBS: 25 mM Tris-HCl, pH 7.4, 150 mM NaCl) containing protease inhibitor mixture (Sigma-Aldrich) and centrifuged at 18,800 × *g* for 60 min at 4 °C, and supernatants were collected (representing the TBS-soluble fraction). Resulting pellets were treated with TNE buffer (10 mM Tris-HCl, 1% Nonidet P-40, 1 mM EDTA, and 150 mM NaCl) with protease inhibitors and homogenized using TissueLyser LT. Homogenates were then centrifuged at 18,800 × *g* for 30 min at 4 °C, and supernatants were collected (representing the detergent-soluble fraction). Remaining pellets were treated with 5 M guanidine HCl and dissolved by occasional mixing on ice for 30 min and centrifuged at 18,800 × *g* for 30 min at 4 °C. Supernatants were then collected; this is taken as the guanidine HCl-soluble fraction. A$\beta_{1\text{-}40}$ and A$\beta_{1\text{-}42}$ species were separately quantified in each sample in duplicate by sandwich ELISA (IBL, Gunma, Japan) (82). Aβ oligomers were quantified in the TNE-soluble fraction in duplicate by human Aβ oligomers (82E1-specific) assay (IBL) (83). All samples fell within the linear range of the standard curve.

Western blotting

Brain homogenates were lysed using TissueLyser LT in TBS containing protease inhibitor mixture (Sigma-Aldrich) followed by TNE buffer. Homogenates were then centrifuged at 18,800 × *g* for 30 min at 4 °C, supernatants were collected, and aliquots corresponding to 10 μg of total protein were electrophoretically separated using Tris glycine gels. Electrophoresed proteins were transferred to polyvinylidene difluoride membranes (Bio-Rad) that were blocked at ambient temperature for 1 h. Membranes were then hybridized at ambient temperature for 1 h with primary antibodies as follows: N-terminal anti-APP pAb (1:2,000; IBL); C-terminal anti-PS1 mAb (1:500; PS1-loop, Merck, Darmstadt, Germany); C-terminal anti-sAPP-α mAb (1:300; 2B3; IBL); C-terminal anti-sAPP-β-sw mAb (1:100; 6A1; IBL); N-terminal anti-A$\beta_{1\text{-}16}$ mAb (1:500; 82E1; IBL); C-terminal anti-ADAM10 pAb (1:1,500; Cell Signaling Technology, Danvers, MA, USA); C-terminal anti-BACE1 pAb (1:400; IBL); anti-furin pAb (1:1,000; Bioss Antibodies Inc., Woburn, MA, USA); anti-Cu/Zn SOD pAb (1:3,000; Enzo Life Sciences, Farmingdale, NY, USA); anti-GPx1 pAb (1:4,000; Boster Biological Technology, Pleasanton, CA, USA), or anti-β-actin mAb (1:5,000; 13E5; Cell Signaling Technology; as a loading control). Membranes were then rinsed and incubated at ambient temperature for 1 h with appropriate horseradish peroxidase-conjugated secondary antibodies. After additional rinsing, membranes were incubated at ambient temperature for 5 min with enhanced chemiluminescence substrate (SuperSignal West Dura Extended Duration Substrate, Thermo Fisher Scientific, Waltham, MA, USA), exposed to film, and developed. Western blots were done for each brain (n = 6, three mice of each sex per group), and quantitative data were averaged.

The α- and β-secretase activity assays

To determine α- and β-secretase activity in brain homogenates, we used available assay kits according to our published methods (2, 4). Briefly, for α-secretase activity (SensoLyte® 520 TACE (α-Secretase) Activity Assay Kit, Anaspec, Inc., Fremont,

CA, USA), brains were lysed using TissueLyser LT in ice-cold 3× volume of extraction buffer containing 1% Nonidet P-40 and centrifuged at 2,000 × *g* for 15 min. For β-secretase activity (β-Secretase Activity Fluorometric Assay Kit, BioVision Inc., Milpitas, CA, USA), brains were lysed using TissueLyser LT in ice-cold 3× volume of extraction buffer and centrifuged at 10,000 × *g* for 5 min. Subsequently, both supernatants were collected and kept on ice. Appropriate amounts of brain homogenate, assay buffer, and substrate were added in duplicate to a 96-well-plate and incubated in the dark at 25 °C for α-secretase activity assays and 37 °C for β-secretase activity assays for kinetics analyses. Following incubation, fluorescence was monitored (490 nm excitation and 520 nm emission for α-secretase activity; 345 nm excitation and 450 nm emission for β-secretase activity) at 25 °C at 0, 15, 30, 45, and 60 min using a SH-9000 microplate fluorimeter with SF6 software (CORONA ELECTRIC, Hitachinaka, Ibaraki, Japan). Background was determined from negative controls (omission of brain homogenate or fluorogenic substrate).

Cell-free β-secretase inhibitor assay

To directly test the effect of GA on β-secretase activity, we used an available assay based on secretase-specific peptides conjugated to DABCYL/EDANS fluorogenic reporter molecules (Cayman Chemical, Ann Arbor, MI, USA) in accordance with the manufacturer's instructions. Briefly, β-secretase (human recombinant) was incubated with various concentrations of GA (1.563, 3.125, 6.25, 12.5, or 25 μM) or β-secretase inhibitor II (1.25 μM, as a positive control; Merck, Darmstadt, Germany) in the presence of assay buffer and fluorogenic substrate for 40 min at room temperature prior to reading fluorescence values. Following incubation, fluorescence was monitored (335-345 nm excitation and 485-510 nm emission) at 25 °C using a SH-9000 microplate fluorimeter with SF6 software (CORONA ELECTRIC). Background was determined from negative controls (*i.e.* assay buffer and solvent).

Q-PCR

We quantified brain *Adam10*, *Bace1*, and *β-actin* mRNA abundance by q-PCR. Total RNA was extracted using the RNeasy Mini Kit (Qiagen), and first-strand cDNA synthesis was carried out using the QuantiTect Reverse Transcription Kit (Qiagen) in accordance with the manufacturer's instructions. We diluted cDNA 1:1 in H_2O and performed q-PCR analysis for all genes of interest using cDNA-specific TaqMan primer/probe sets (TaqMan Gene Expression Assays, Thermo Fisher Scientific) on an ABI 7500 Fast Real-time PCR instrument (Thermo Fisher Scientific). Each 20-μl reaction mixture contained 2 μl of cDNA with 1 μl of TaqMan Gene Expression Assay reagent, 10 μl of TaqMan Fast Advanced Master Mix (Thermo Fisher Scientific), and 7 μl of H_2O. Thermocycler conditions consisted of 95 °C for 15 s, followed by 40 cycles of 95 °C for 1 s and 60 °C for 20 s. TaqMan probe/primer sets were *Bace1* (number Mm00478664_m1), *Adam10* (number Mm00545742_m1), and *β-actin* (number Mm00607939_s1; used as an internal reference control) (Thermo Fisher Scientific). Samples that were not subjected to reverse transcription were run in parallel as negative controls to rule out genomic DNA contamination, and a no template control was also included for each primer set. The cycle threshold number (C_T) method (84) was used to determine relative amounts of initial target cDNA in each sample. Results are expressed relative to vehicle-treated WT mouse brains.

Statistical analysis

Data are presented as mean ± S.D. A hierarchical analysis strategy was used in which we first conducted an overall ANOVA (repeated measures was used for behavioral data) to assess significance of main effects and interactive terms. If the model was significant, post hoc testing was done with Tukey's HSD or Dunnett's T3 methods, where appropriateness was determined based on Levene's test for equality of the variance. In instances of multiple mean comparisons, one-way ANOVA was used, followed by post hoc comparison of the means using Bonferroni's or Dunnett's T3 methods (depending on Levene's test for equality of the variance). The α levels were set at 0.05 for all analyses. All analyses were performed using the Statistical Package for the Social Sciences, release 23.0 (IBM SPSS, Armonk, NY, USA).

Data availability

All data described in this manuscript are contained within the manuscript.

Author contributions—T. M. and T. T. conceptualized the study; T. M. and T. T. analyzed data; T. M., N. K., T. Y., D. S., J. T., T. S., and M. M. performed experiments; T. M. and T. T. wrote the draft; T. M. and T. T. administered the project; T. M. and T. T. reviewed and edited the draft.

Funding and additional information—This work was supported, in whole or in part, by National Institutes of Health Grants 2R01NS076794-06A1, 1RF1AG053982-01A1, 5P01AG052350-03, and 5R21AG053884-02 (to T. T.), Japan Society for the Promotion of Science Grant KAKENHI JP26430058 (to T. M.), an Alzheimer's Association Sex and Gender in Alzheimer's Disease Grant (SAGA; to T. T.), Cure Alzheimer's Fund (to T. T.), and a Coins for Alzheimer's Research Trust Grant (to T. T). The content is solely the responsibility of the authors and does not necessarily represent the official views of the National Institutes of Health.

Conflict of interest—The authors declare that they have no conflicts of interest with the contents of this article.

Abbreviations—The abbreviations used are: AD, Alzheimer's disease; Aβ, amyloid β-protein; GA, gallic acid; APP/PS1, mutant human amyloid β-protein precursor/presenilin 1; RAWM, radial arm water maze; ANOVA, analysis of variance; RSC, retrosplenial cortex; EC, entorhinal cortex; H, hippocampus; ROI, regions of interest; CAA, cerebral amyloid angiopathy; sAPP, soluble APP; β-CTF/C99, β-C-terminal APP fragment; P-β-CTF/P-C99, phospho-β-CTF; BACE1, β-site APP-cleaving enzyme 1; ADAM10, a disintegrin and metalloproteinase domain-containing protein 10; pADAM10, precursor ADAM10; mADAM10, mature (active) ADAM10; q-PCR, quantitative real-time PCR; GFAP, glial fibrillary

acidic protein; Iba1, ionized calcium-binding adapter molecule 1; SOD1, superoxide dismutase 1; GPx1, GSH peroxidase 1; NOAEL, no observed adverse effect level.

References

1. Selkoe, D. J. (2001) Alzheimer's disease: genes, proteins, and therapy. *Physiol. Rev.* **81,** 741–766 CrossRef Medline
2. Rezai-Zadeh, K., Shytle, D., Sun, N., Mori, T., Hou, H., Jeanniton, D., Ehrhart, J., Townsend, K., Zeng, J., Morgan, D., Hardy, J., Town, T., and Tan, J. (2005) Green tea epigallocatechin-3-gallate (EGCG) modulates amyloid precursor protein cleavage and reduces cerebral amyloidosis in Alzheimer transgenic mice. *J. Neurosci.* **25,** 8807–8814 CrossRef Medline
3. Obregon, D. F., Rezai-Zadeh, K., Bai, Y., Sun, N., Hou, H., Ehrhart, J., Zeng, J., Mori, T., Arendash, G. W., Shytle, D., Town, T., and Tan, J. (2006) ADAM10 activation is required for green tea (−)-epigallocatechin-3-gallate-induced α-secretase cleavage of amyloid precursor protein. *J. Biol. Chem.* **281,** 16419–16427 CrossRef Medline
4. Mori, T., Rezai-Zadeh, K., Koyama, N., Arendash, G. W., Yamaguchi, H., Kakuda, N., Horikoshi-Sakuraba, Y., Tan, J., and Town, T. (2012) Tannic acid is a natural β-secretase inhibitor that prevents cognitive impairment and mitigates Alzheimer-like pathology in transgenic mice. *J. Biol. Chem.* **287,** 6912–6927 CrossRef Medline
5. Zhang, S. Q., Sawmiller, D., Li, S., Rezai-Zadeh, K., Hou, H., Zhou, S., Shytle, D., Giunta, B., Fernandez, F., Mori, T., and Tan, J. (2013) Octyl gallate markedly promotes anti-amyloidogenic processing of APP through estrogen receptor-mediated ADAM10 activation. *PLoS ONE* **8,** e71913 CrossRef Medline
6. Liu, Y., Pukala, T. L., Musgrave, I. F., Williams, D. M., Dehle, F. C., and Carver, J. A. (2013) Gallic acid is the major component of grape seed extract that inhibits amyloid fibril formation. *Bioorg. Med. Chem. Lett.* **23,** 6336–6340 CrossRef Medline
7. Yu, M., Chen, X., Liu, J., Ma, Q., Zhuo, Z., Chen, H., Zhou, L., Yang, S., Zheng, L., Ning, C., Xu, J., Gao, T., and Hou, S. T. (2019) Gallic acid disruption of $A\beta_{1\text{-}42}$ aggregation rescues cognitive decline of APP/PS1 double transgenic mouse. *Neurobiol. Dis.* **124,** 67–80 CrossRef Medline
8. Hajipour, S., Sarkaki, A., Farbood, Y., Eidi, A., Mortazavi, P., and Valizadeh, Z. (2016) Effect of gallic acid on dementia type of Alzheimer disease in rats: electrophysiological and histological studies. *Basic. Clin. Neurosci.* **7,** 97–106 Medline
9. Kim, M. J., Seong, A. R., Yoo, J. Y., Jin, C. H., Lee, Y. H., Kim, Y. J., Lee, J., Jun, W. J., and Yoon, H. G. (2011) Gallic acid, a histone acetyltransferase inhibitor, suppresses β-amyloid neurotoxicity by inhibiting microglial-mediated neuroinflammation. *Mol. Nutr. Food Res.* **55,** 1798–1808 CrossRef Medline
10. Serrano, J., Puupponen-Pimiä, R., Dauer, A., Aura, A. M., and Saura-Calixto, F. (2009) Tannins: current knowledge of food sources, intake, bioavailability and biological effects. *Mol. Nutr. Food Res.* **53,** S310–S329 CrossRef Medline
11. Fernandes, F. H., and Salgado, H. R. (2016) Gallic acid: review of the methods of determination and quantification. *Crit. Rev. Anal. Chem.* **46,** 257–265 CrossRef Medline
12. Kim, Y. J. (2007) Antimelanogenic and antioxidant properties of gallic acid. *Biol. Pharm. Bull.* **30,** 1052–1055 CrossRef Medline
13. Punithavathi, V. R., Prince, P. S., Kumar, R., and Selvakumari, J. (2011) Antihyperglycaemic, antilipid peroxidative and antioxidant effects of gallic acid on streptozotocin induced diabetic Wistar rats. *Eur. J. Pharmacol.* **650,** 465–471 CrossRef Medline
14. Verma, S., Singh, A., and Mishra, A. (2013) Gallic acid: molecular rival of cancer. *Environ. Toxicol. Pharmacol.* **35,** 473–485 CrossRef Medline
15. Kratz, J. M., Andrighetti-Fröhner, C. R., Kolling, D. J., Leal, P. C., Cirne-Santos, C. C., Yunes, R. A., Nunes, R. J., Trybala, E., Bergström, T., Frugulhetti, I. C., Barardi, C. R., and Simões, C. M. (2008) Anti-HSV-1 and anti-HIV-1 activity of gallic acid and pentyl gallate. *Mem. Inst. Oswaldo. Cruz.* **103,** 437–442 CrossRef Medline
16. Jung, J., Bae, K. H., and Jeong, C. S. (2013) Anti-*Helicobacter pylori* and antiulcerogenic activities of the root cortex of *Paeonia suffruticosa*. *Biol. Pharm. Bull.* **36,** 1535–1539 CrossRef Medline
17. Dhingra, D., Chhillar, R., and Gupta, A. (2012) Antianxiety-like activity of gallic acid in unstressed and stressed mice: possible involvement of nitriergic system. *Neurochem. Res.* **37,** 487–494 CrossRef Medline
18. Chhillar, R., and Dhingra, D. (2013) Antidepressant-like activity of gallic acid in mice subjected to unpredictable chronic mild stress. *Fundam. Clin. Pharmacol.* **27,** 409–418 CrossRef Medline
19. Huang, H. L., Lin, C. C., Jeng, K. C., Yao, P. W., Chuang, L. T., Kuo, S. L., and Hou, C. W. (2012) Fresh green tea and gallic acid ameliorate oxidative stress in kainic acid-induced status epilepticus. *J. Agric. Food Chem.* **60,** 2328–2336 CrossRef Medline
20. Korani, M. S., Farbood, Y., Sarkaki, A., Fathi Moghaddam, H., and Taghi Mansouri, M. (2014) Protective effects of gallic acid against chronic cerebral hypoperfusion-induced cognitive deficit and brain oxidative damage in rats. *Eur. J. Pharmacol.* **733,** 62–67 CrossRef Medline
21. Arendash, G. W., King, D. L., Gordon, M. N., Morgan, D., Hatcher, J. M., Hope, C. E., and Diamond, D. M. (2001) Progressive, age-related behavioral impairments in transgenic mice carrying both mutant amyloid precursor protein and presenilin-1 transgenes. *Brain Res.* **891,** 42–53 CrossRef Medline
22. King, D. L., Arendash, G. W., Crawford, F., Sterk, T., Menendez, J., and Mullan, M. J. (1999) Progressive and gender-dependent cognitive impairment in the APP_{SW} transgenic mouse model for Alzheimer's disease. *Behav. Brain Res.* **103,** 145–162 CrossRef
23. Town, T., Laouar, Y., Pittenger, C., Mori, T., Szekely, C. A., Tan, J., Duman, R. S., and Flavell, R. A. (2008) Blocking TGF-β-Smad2/3 innate immune signaling mitigates Alzheimer-like pathology. *Nat. Med.* **14,** 681–687 CrossRef Medline
24. Mori, T., Koyama, N., Guillot-Sestier, M. V., Tan, J., and Town, T. (2013) Ferulic acid is a nutraceutical β-secretase modulator that improves behavioral impairment and Alzheimer-like pathology in transgenic mice. *PLoS ONE* **8,** e55774 CrossRef Medline
25. Mori, T., Koyama, N., Segawa, T., Maeda, M., Maruyama, N., Kinoshita, N., Hou, H., Tan, J., and Town, T. (2014) Methylene blue modulates β-secretase, reverses cerebral amyloidosis, and improves cognition in transgenic mice. *J. Biol. Chem.* **289,** 30303–30317 CrossRef Medline
26. Mori, T., Koyama, N., Tan, J., Segawa, T., Maeda, M., and Town, T. (2017) Combination therapy with octyl gallate and ferulic acid improves cognition and neurodegeneration in a transgenic mouse model of Alzheimer disease. *J. Biol. Chem.* **292,** 11310–11325 CrossRef
27. Mori, T., Koyama, N., Tan, J., Segawa, T., Maeda, M., and Town, T. (2019) Combined treatment with the phenolics (−)-epigallocatechin-3-gallate and ferulic acid improves cognition and reduces Alzheimer-like pathology in mice. *J. Biol. Chem.* **294,** 2714–2731 CrossRef Medline
28. Kim, K. S., and Han, P. L. (2006) Optimization of chronic stress paradigms using anxiety- and depression-like behavioral parameters. *J. Neurosci. Res.* **83,** 497–507 CrossRef Medline
29. Ellis, R. J., Olichney, J. M., Thal, L. J., Mirra, S. S., Morris, J. C., Beekly, D., and Heyman, A. (1996) Cerebral amyloid angiopathy in the brains of patients with Alzheimer's disease: the CERAD experience, part XV. *Neurology* **46,** 1592–1596 CrossRef Medline
30. DeMattos, R. B., Bales, K. R., Cummins, D. J., Paul, S. M., and Holtzman, D. M. (2002) Brain to plasma amyloid-β efflux: a measure of brain amyloid burden in a mouse model of Alzheimer's disease. *Science* **295,** 2264–2267 CrossRef Medline
31. Vincent, B. (2016) Regulation of the α-secretase ADAM10 at transcriptional, translational and post-translational levels. *Brain Res. Bull.* **126,** 154–169 CrossRef Medline
32. Rajalakshmi, K., Devaraj, H., and Niranjali Devaraj, S. (2001) Assessment of the no-observed-adverse-effect level (NOAEL) of gallic acid in mice. *Food Chem. Toxicol.* **39,** 919–922 CrossRef Medline
33. Barnes, D. G., and Dourson, M. (1988) Reference dose (RfD): description and use in health risk assessments. *Regul. Toxicol. Pharmacol.* **8,** 471–486 CrossRef Medline

34. Environmental Health Criteria, 210 (1999) Principles for the assessment of risks to human health from exposure chemicals. http://www.inchem.org/documents/ehc/ehc/ehc210.htm
35. Reagan-Shaw, S., Nihal, M., and Ahmad, N. (2008) Dose translation from animal to human studies revisited. *FASEB J.* **22,** 659–661 CrossRef Medline
36. Konishi, Y., Hitomi, Y., and Yoshioka, E. (2004) Intestinal absorption of p-coumaric and gallic acids in rats after oral administration. *J. Agric. Food Chem.* **52,** 2527–2532 CrossRef Medline
37. Shahrzad, S., Aoyagi, K., Winter, A., Koyama, A., and Bitsch, I. (2001) Pharmacokinetics of gallic acid and its relative bioavailability from tea in healthy humans. *J. Nutr.* **131,** 1207–1210 CrossRef Medline
38. Konishi, Y., Zhao, Z., and Shimizu, M. (2006) Phenolic acids are absorbed from the rat stomach with different absorption rates. *J. Agric. Food Chem.* **54,** 7539–7543 CrossRef Medline
39. Ferruzzi, M. G., Lobo, J. K., Janle, E. M., Cooper, B., Simon, J. E., Wu, Q. L., Welch, C., Ho, L., Weaver, C., and Pasinetti, G. M. (2009) Bioavailability of gallic acid and catechins from grape seed extract is improved by repeated dosing in rats: implications for treatment in Alzheimer's disease. *J. Alzheimers Dis.* **18,** 113–124 CrossRef Medline
40. De Strooper, B., Saftig, P., Craessaerts, K., Vanderstichele, H., Guhde, G., Annaert, W., Von Figura, K., and Van Leuven, F. (1998) Deficiency of presenilin-1 inhibits the normal cleavage of amyloid precursor protein. *Nature* **391,** 387–390 CrossRef Medline
41. Sinha, S., and Lieberburg, I. (1999) Cellular mechanisms of β-amyloid production and secretion. *Proc. Natl. Acad. Sci. U.S.A.* **96,** 11049–11053 CrossRef Medline
42. Vassar, R., Bennett, B. D., Babu-Khan, S., Kahn, S., Mendiaz, E. A., Denis, P., Teplow, D. B., Ross, S., Amarante, P., Loeloff, R., Luo, Y., Fisher, S., Fuller, J., Edenson, S., Lile, J., *et al.* (1999) β-Secretase cleavage of Alzheimer's amyloid precursor protein by the transmembrane aspartic protease BACE. *Science* **286,** 735–741 CrossRef Medline
43. Kimberly, W. T., LaVoie, M. J., Ostaszewski, B. L., Ye, W., Wolfe, M. S., and Selkoe, D. J. (2003) γ-Secretase is a membrane protein complex comprised of presenilin, nicastrin, Aph-1, and Pen-2. *Proc. Natl. Acad. Sci. U.S.A.* **100,** 6382–6387 CrossRef Medline
44. Postina, R., Schroeder, A., Dewachter, I., Bohl, J., Schmitt, U., Kojro, E., Prinzen, C., Endres, K., Hiemke, C., Blessing, M., Flamez, P., Dequenne, A., Godaux, E., van Leuven, F., and Fahrenholz, F. (2004) A disintegrin-metalloproteinase prevents amyloid plaque formation and hippocampal defects in an Alzheimer disease mouse model. *J. Clin. Invest.* **113,** 1456–1464 CrossRef Medline
45. Mattson, M. P., Cheng, B., Culwell, A. R., Esch, F. S., Lieberburg, I., and Rydel, R. E. (1993) Evidence for excitoprotective and intraneuronal calcium-regulating roles for secreted forms of the β-amyloid precursor protein. *Neuron* **10,** 243–254 CrossRef Medline
46. Mattson, M. P. (1997) Cellular actions of β-amyloid precursor protein and its soluble and fibrillogenic derivatives. *Physiol. Rev.* **77,** 1081–1132 CrossRef Medline
47. Ishida, A., Furukawa, K., Keller, J. N., and Mattson, M. P. (1997) Secreted form of β-amyloid precursor protein shifts the frequency dependency for induction of LTD, and enhances LTP in hippocampal slices. *Neuroreport* **8,** 2133–2137 CrossRef Medline
48. Obregon, D., Hou, H., Deng, J., Giunta, B., Tian, J., Darlington, D., Shahaduzzaman, M., Zhu, Y., Mori, T., Mattson, M. P., and Tan, J. (2012) Soluble amyloid precursor protein-α modulates β-secretase activity and amyloid-β generation. *Nat. Commun.* **3,** 777 CrossRef Medline
49. Kaden, D., Munter, L. M., Joshi, M., Treiber, C., Weise, C., Bethge, T., Voigt, P., Schaefer, M., Beyermann, M., Reif, B., and Multhaup, G. (2008) Homophilic interactions of the amyloid precursor protein (APP) ectodomain are regulated by the loop region and affect β-secretase cleavage of APP. *J. Biol. Chem.* **283,** 7271–7279 CrossRef Medline
50. Young-Pearse, T. L., Chen, A. C., Chang, R., Marquez, C., and Selkoe, D. J. (2008) Secreted APP regulates the function of full-length APP in neurite outgrowth through interaction with integrin β1. *Neural. Dev.* **3,** 15 CrossRef Medline
51. Gralle, M., Botelho, M. G., and Wouters, F. S. (2009) Neuroprotective secreted amyloid precursor protein acts by disrupting amyloid precursor protein dimers. *J. Biol. Chem.* **284,** 15016–15025 CrossRef Medline
52. Sabbagh, M. N., Cooper, K., DeLange, J., Stoehr, J. D., Thind, K., Lahti, T., Reisberg, B., Sue, L., Vedders, L., Fleming, S. R., and Beach, T. G. (2010) Functional, global and cognitive decline correlates to accumulation of Alzheimer's pathology in MCI and AD. *Curr. Alzheimer Res.* **7,** 280–286 CrossRef Medline
53. Robinson, J. L., Geser, F., Corrada, M. M., Berlau, D. J., Arnold, S. E., Lee, V. M., Kawas, C. H., and Trojanowski, J. Q. (2011) Neocortical and hippocampal amyloid-β and tau measures associate with dementia in the oldest-old. *Brain* **134,** 3708–3715 CrossRef Medline
54. Price, J. L., McKeel, D. W., Jr., Buckles, V. D., Roe, C. M., Xiong, C., Grundman, M., Hansen, L. A., Petersen, R. C., Parisi, J. E., Dickson, D. W., Smith, C. D., Davis, D. G., Schmitt, F. A., Markesbery, W. R., Kaye, J., *et al.* (2009) Neuropathology of nondemented aging: presumptive evidence for preclinical Alzheimer disease. *Neurobiol. Aging* **30,** 1026–1036 CrossRef Medline
55. Mufson, E. J., Malek-Ahmadi, M., Perez, S. E., and Chen, K. (2016) Braak staging, plaque pathology, and APOE status in elderly persons without cognitive impairment. *Neurobiol. Aging* **37,** 147–153 CrossRef Medline
56. Schenk, D., Barbour, R., Dunn, W., Gordon, G., Grajeda, H., Guido, T., Hu, K., Huang, J., Johnson-Wood, K., Khan, K., Kholodenko, D., Lee, M., Liao, Z., Lieberburg, I., Motter, R., *et al.* (1999) Immunization with amyloid-β attenuates Alzheimer-disease-like pathology in the PDAPP mouse. *Nature* **400,** 173–177 CrossRef Medline
57. Kotilinek, L. A., Bacskai, B., Westerman, M., Kawarabayashi, T., Younkin, L., Hyman, B. T., Younkin, S., and Ashe, K. H. (2002) Reversible memory loss in a mouse transgenic model of Alzheimer's disease. *J. Neurosci.* **22,** 6331–6335 CrossRef Medline
58. Hartman, R. E., Izumi, Y., Bales, K. R., Paul, S. M., Wozniak, D. F., and Holtzman, D. M. (2005) Treatment with an amyloid-β antibody ameliorates plaque load, learning deficits, and hippocampal long-term potentiation in a mouse model of Alzheimer's disease. *J. Neurosci.* **25,** 6213–6220 CrossRef Medline
59. Mouri, A., Noda, Y., Hara, H., Mizoguchi, H., Tabira, T., and Nabeshima, T. (2007) Oral vaccination with a viral vector containing Aβ cDNA attenuates age-related Aβ accumulation and memory deficits without causing inflammation in a mouse Alzheimer model. *FASEB J.* **21,** 2135–2148 CrossRef Medline
60. Holcomb, L. A., Gordon, M. N., Jantzen, P., Hsiao, K., Duff, K., and Morgan, D. (1999) Behavioral changes in transgenic mice expressing both amyloid precursor protein and presenilin-1 mutations: lack of association with amyloid deposits. *Behav. Genet.* **29,** 177–185 CrossRef Medline
61. Westerman, M. A., Cooper-Blacketer, D., Mariash, A., Kotilinek, L., Kawarabayashi, T., Younkin, L. H., Carlson, G. A., Younkin, S. G., and Ashe, K. H. (2002) The relationship between Aβ and memory in the Tg2576 mouse model of Alzheimer's disease. *J. Neurosci.* **22,** 1858–1867 CrossRef Medline
62. Walsh, D. M., Klyubin, I., Fadeeva, J. V., Cullen, W. K., Anwyl, R., Wolfe, M. S., Rowan, M. J., and Selkoe, D. J. (2002) Naturally secreted oligomers of amyloid β protein potently inhibit hippocampal long-term potentiation *in vivo*. *Nature* **416,** 535–539 CrossRef Medline
63. Cleary, J. P., Walsh, D. M., Hofmeister, J. J., Shankar, G. M., Kuskowski, M. A., Selkoe, D. J., and Ashe, K. H. (2005) Natural oligomers of the amyloid-β protein specifically disrupt cognitive function. *Nat. Neurosci.* **8,** 79–84 CrossRef Medline
64. Haass, C., and Selkoe, D. J. (2007) Soluble protein oligomers in neurodegeneration: lessons from the Alzheimer's amyloid β-peptide. *Nat. Rev. Mol. Cell Biol.* **8,** 101–112 CrossRef Medline
65. Shankar, G. M., Li, S., Mehta, T. H., Garcia-Munoz, A., Shepardson, N. E., Smith, I., Brett, F. M., Farrell, M. A., Rowan, M. J., Lemere, C. A., Regan, C. M., Walsh, D. M., Sabatini, B. L., and Selkoe, D. J. (2008) Amyloid-β protein dimers isolated directly from Alzheimer's brains impair synaptic plasticity and memory. *Nat. Med.* **14,** 837–842 CrossRef Medline
66. Griffin, W. S., Sheng, J. G., Royston, M. C., Gentleman, S. M., McKenzie, J. E., Graham, D. I., Roberts, G. W., and Mrak, R. E. (1998) Glial-neuronal interactions in Alzheimer's disease: the potential role of a "cytokine cycle" in disease progression. *Brain Pathol.* **8,** 65–72 CrossRef Medline

67. Akiyama, H., Barger, S., Barnum, S., Bradt, B., Bauer, J., Cole, G. M., Cooper, N. R., Eikelenboom, P., Emmerling, M., Fiebich, B. L., Finch, C. E., Frautschy, S., Griffin, W. S., Hampel, H., Hull, M., *et al.* (2000) Inflammation and Alzheimer's disease. *Neurobiol. Aging* **21,** 383–421 CrossRef Medline
68. Heneka, M. T., Carson, M. J., El Khoury, J., Landreth, G. E., Brosseron, F., Feinstein, D. L., Jacobs, A. H., Wyss-Coray, T., Vitorica, J., Ransohoff, R. M., Herrup, K., Frautschy, S. A., Finsen, B., Brown, G. C., Verkhratsky, A., *et al.* (2015) Neuroinflammation in Alzheimer's disease. *Lancet Neurol.* **14,** 388–405 CrossRef Medline
69. Andreasson, K. I., Bachstetter, A. D., Colonna, M., Ginhoux, F., Holmes, C., Lamb, B., Landreth, G., Lee, D. C., Low, D., Lynch, M. A., Monsonego, A., O'Banion, M. K., Pekny, M., Puschmann, T., Russek-Blum, N., *et al.* (2016) Targeting innate immunity for neurodegenerative disorders of the central nervous system. *J. Neurochem.* **138,** 653–693 CrossRef Medline
70. Ridet, J. L., Malhotra, S. K., Privat, A., and Gage, F. H. (1997) Reactive astrocytes: cellular and molecular cues to biological function. *Trends Neurosci.* **20,** 570–577 CrossRef Medline
71. Tan, J., Town, T., Crawford, F., Mori, T., DelleDonne, A., Crescentini, R., Obregon, D., Flavell, R. A., and Mullan, M. J. (2002) Role of CD40 ligand in amyloidosis in transgenic Alzheimer's mice. *Nat. Neurosci.* **5,** 1288–1293 CrossRef Medline
72. Town, T., Nikolic, V., and Tan, J. (2005) The microglial "activation" continuum: from innate to adaptive responses. *J. Neuroinflammation* **2,** 24 CrossRef Medline
73. Valko, M., Leibfritz, D., Moncol, J., Cronin, M. T., Mazur, M., and Telser, J. (2007) Free radicals and antioxidants in normal physiological functions and human disease. *Int. J. Biochem. Cell Biol.* **39,** 44–84 CrossRef Medline
74. Murphy, M. P. (2009) How mitochondria produce reactive oxygen species. *Biochem. J.* **417,** 1–13 CrossRef Medline
75. Yan, S. D., Chen, X., Fu, J., Chen, M., Zhu, H., Roher, A., Slattery, T., Zhao, L., Nagashima, M., Morser, J., Migheli, A., Nawroth, P., Stern, D., and Schmidt, A. M. (1996) RAGE and amyloid-β peptide neurotoxicity in Alzheimer's disease. *Nature* **382,** 685–691 CrossRef Medline
76. Markesbery, W. R. (1997) Oxidative stress hypothesis in Alzheimer's disease. *Free Radic. Biol. Med.* **23,** 134–147 CrossRef Medline
77. Jankowsky, J. L., Slunt, H. H., Gonzales, V., Jenkins, N. A., Copeland, N. G., and Borchelt, D. R. (2004) APP processing and amyloid deposition in mice haplo-insufficient for presenilin 1. *Neurobiol. Aging* **25,** 885–892 CrossRef Medline
78. De Rosa, R., Garcia, A. A., Braschi, C., Capsoni, S., Maffei, L., Berardi, N., and Cattaneo, A. (2005) Intranasal administration of nerve growth factor (NGF) rescues recognition memory deficits in AD11 anti-NGF transgenic mice. *Proc. Natl. Acad. Sci. U.S.A.* **102,** 3811–3816 CrossRef Medline
79. Alamed, J., Wilcock, D. M., Diamond, D. M., Gordon, M. N., and Morgan, D. (2006) Two-day radial-arm water maze learning and memory task; robust resolution of amyloid-related memory deficits in transgenic mice. *Nat. Protoc.* **1,** 1671–1679 CrossRef Medline
80. Franklin, K. B. J., and Paxinos, G. (2001) *The Mouse Brain in Stereotaxic Coordinates*, Academic Press, San Diego
81. Kawarabayashi, T., Younkin, L. H., Saido, T. C., Shoji, M., Ashe, K. H., and Younkin, S. G. (2001) Age-dependent changes in brain, CSF, and plasma amyloid (β) protein in the Tg2576 transgenic mouse model of Alzheimer's disease. *J. Neurosci.* **21,** 372–381 CrossRef Medline
82. Horikoshi, Y., Sakaguchi, G., Becker, A. G., Gray, A. J., Duff, K., Aisen, P. S., Yamaguchi, H., Maeda, M., Kinoshita, N., and Matsuoka, Y. (2004) Development of Aβ terminal end-specific antibodies and sensitive ELISA for Aβ variant. *Biochem. Biophys. Res. Commun.* **319,** 733–737 CrossRef Medline
83. Xia, W., Yang, T., Shankar, G., Smith, I. M., Shen, Y., Walsh, D. M., and Selkoe, D. J. (2009) A specific enzyme-linked immunosorbent assay for measuring β-amyloid protein oligomers in human plasma and brain tissue of patients with Alzheimer disease. *Arch. Neurol.* **66,** 190–199 CrossRef Medline
84. Monney, L., Sabatos, C. A., Gaglia, J. L., Ryu, A., Waldner, H., Chernova, T., Manning, S., Greenfield, E. A., Coyle, A. J., Sobel, R. A., Freeman, G. J., and Kuchroo, V. K. (2002) Th1-specific cell surface protein Tim-3 regulates macrophage activation and severity of an autoimmune disease. *Nature* **415,** 536–541 CrossRef Medline